NEOPLASIA
www.neoplasia.com

Volume 15 Number 8 August 2013 pp. 898–912 898

A Novel Mechanism for CTCF in the Epigenetic Regulation of *Bax* in Breast Cancer Cells[1,2]

Claudia Fabiola Méndez-Catalá[*,3], Svetlana Gretton[*,3], Alexander Vostrov[†], Elena Pugacheva[†], Dawn Farrar[*], Yoko Ito[‡], France Docquier[§], Georgia-Xanthi Kita[*], Adele Murrell[‡], Victor Lobanenkov[†] and Elena Klenova[*]

*School of Biological Sciences, University of Essex, Colchester, Essex, United Kingdom; [†]Molecular Pathology Section, Laboratory of Immunopathology, National Institute of Allergy and Infectious Diseases, National Institutes of Health, Rockville, MD; [‡]Cancer Research UK Cambridge Research Institute, Cambridge, United Kingdom; [§]Helen Rollason Research Laboratory, PMI 208, Postgraduate Medical Institute (PMI), Anglia Ruskin University, Chelmsford, Essex, United Kingdom

Abstract

We previously reported the association of elevated levels of the multifunctional transcription factor, CCCTC binding factor (CTCF), in breast cancer cells with the specific anti-apoptotic function of CTCF. To understand the molecular mechanisms of this phenomenon, we investigated regulation of the human *Bax* gene by CTCF in breast and non–breast cells. Two CTCF binding sites (CTSs) within the *Bax* promoter were identified. In all cells, breast and non-breast, active histone modifications were present at these CTSs, DNA harboring this region was unmethylated, and levels of *Bax* mRNA and protein were similar. Nevertheless, up-regulation of *Bax* mRNA and protein and apoptotic cell death were observed only in breast cancer cells depleted of CTCF. We proposed that increased CTCF binding to the *Bax* promoter in breast cancer cells, by comparison with non–breast cells, may be mechanistically linked to the specific apoptotic phenotype in CTCF-depleted breast cancer cells. In this study, we show that CTCF binding was enriched at the *Bax* CTSs in breast cancer cells and tumors; in contrast, binding of other transcription factors (SP1, WT1, EGR1, and c-Myc) was generally increased in non–breast cells and normal breast tissues. Our findings suggest a novel mechanism for CTCF in the epigenetic regulation of *Bax* in breast cancer cells, whereby elevated levels of CTCF support preferential binding of CTCF to the *Bax* CTSs. In this context, CTCF functions as a transcriptional repressor counteracting influences of positive regulatory factors; depletion of breast cancer cells from CTCF therefore results in the activation of *Bax* and apoptosis.

Neoplasia (2013) 15, 898–912

Abbreviations: CTCF, CCCTC binding factor; MTT, microculture tetrazolium test; EMSA, electrophoretic mobility shift assay; RT-qPCR, reverse transcription–quantitative polymerase chain reaction; ChIP, chromatin immunoprecipitation; TUNEL, terminal deoxynucleotidyl transferase–mediated deoxyuridine triphosphate nick end labeling

Address all correspondence to: Elena Klenova, PhD, School of Biological Sciences, University of Essex, Wivenhoe Park, Colchester, Essex CO4 3SQ, United Kingdom.
E-mail: klenovae@essex.ac.uk

[1]This work was supported by the Postgraduate Scholarship from CONACyT, Mexico (C.F.M.-C.), Breast Cancer Campaign (F.D. and E.K.), Breast Cancer Research Trust (G.-X.K. and E.K.), Helen Rollason Cancer Charity (F.D.), Medical Research Council and Cancer Research UK (D.F. and E.K.), Research Promotion Fund from the University of Essex (F.D., D.F., and E.K.), the Intramural Research Program of the National Institutes of Health, National Institute of Allergy and Infectious Diseases (A.V., E.P., and V.L.), Cancer Research UK Senior Cancer Research Fellowship (A.M.), and Association for International Cancer Research (A.M. and Y.I.), as well as the support of the University of Cambridge, Cancer Research UK, and Hutchison Whampoa Limited (A.M. and Y.I.).

[2]This article refers to supplementary materials, which are designated by Figures W1 to W10 and are available online at www.neoplasia.com.

[3]These two authors contributed equally to this work.

Received 21 November 2012; Revised 23 April 2013; Accepted 3 May 2013

DOI 10.1593/neo.121948

Introduction

CCCTC binding factor (CTCF) is a multifunctional, highly conserved, and ubiquitous 11-Zn-finger (ZF) transcription factor binding to numerous highly diverse sequences, usually in a methylation-sensitive manner [1,2]. A growing body of evidence supports the importance of CTCF in the organization of nuclear space [3]. Using different genetic and epigenetic mechanisms, CTCF regulates a wide range of genes associated with tumor development, in particular genes involved in growth, proliferation, differentiation, and apoptosis [1,4–7]. CTCF functions are affected by interactions with protein partners and post-translational modifications [8,9]; in particular, loss of CTCF poly (ADP-ribosyl)ation is linked to breast tumorigenesis [10].

Our previous study revealed that elevated levels of CTCF in breast cancer cell lines and tumors are associated with the resistance to apoptosis in breast cancer cells [11]. Using a proteomics approach, the pro-apoptotic protein Bax was identified as a potential target for regulation by CTCF [11]. The Bcl-2 protein family, of which Bax is a member, plays a critical role in determining either cell death or survival [12,13]. In particular, the balance between Bax (pro-apoptotic) and Bcl-2 (anti-apoptotic) protein levels is important for the regulation of apoptosis [14]. Overexpression of Bax leads to apoptosis in the absence of any stimulus, suggesting that tight regulation of Bax, from transcription to posttranslation, is necessary for cell survival [15]. Transcriptional control of *Bax* is complex, is cell context–dependent, and involves many other transcription factors, e.g., WT1 [16], EGR1 [17], c-Myc [18], and also p53 and p73 [19,20]; the latter two are potent regulators of apoptosis in numerous cellular systems [21]. While the majority of human cancers lack a functional p53 tumor suppressor protein, apoptosis can still occur through p53-independent apoptotic processes [22]. Such p53-independent apoptotic pathways are very important to identify as targets for potential therapeutic interventions.

Loss of function of Bax has been linked to tumorigenesis [23]; this is further exemplified by the studies demonstrating improved survival of patients with Bax-expressing tumors compared with those with no or low Bax expression (for example, [24]). Because mutations in the *Bax* gene have been shown to be very rare [25], epigenetic mechanisms are likely to be involved in differential regulation of Bax in tumors.

In this study, we further investigate the role of CTCF in the transcriptional regulation of *Bax*. We establish a novel function for CTCF in the differential epigenetic regulation of *Bax* in breast and non–breast cells. Our proposed model is based on higher levels of CTCF, in breast cancer cells, that favor CTCF binding to the *Bax* promoter. In this context, CTCF acts as a transcriptional repressor as depletion of CTCF leads to activation of *Bax* and apoptotic cell death.

Materials and Methods

Cells and Human Breast Tissues

Breast (MCF-7, ZR75.1, T47D, and Cama1) and non–breast cell lines (293T, HeLa, LnCap, J82, UTA6, G361, DU145, K562, and derivatives) were maintained as described previously [11,26] and breast cell line SUM159PT as recommended [27]. Primary human tumor tissues together with paired peripheral tissues (referred here as "normal") were collected during surgery from breast cancer patients treated at Colchester General Hospital (Essex, United Kingdom), with written consent taken before surgery. The study was approved by the Local Ethic Committee (Reference No. MH363).

Transfection with siRNA

A panel of siRNAs, Hs_CTCF_1 siRNA through Hs_CTCF_4 and *Bax* siRNA (Qiagen, Manchester, United Kingdom) and CTCF SMARTpool siRNA, non-target siRNA, and *cyclophilin B* siRNA [all three from Dharmacon (Epsom, United Kingdom)], was used at a concentration of 50 pM. Cells were seeded at a density of 2.5×10^5 (MCF-7 and ZR75.1) or 1.2×10^5 (Cama1, 293T, and HeLa) and transfected on the following day with siRNA and DharmaFECT2 (Dharmacon) according to the manufacturer's protocol.

Western Blot Analysis

Lysates from cells and breast tissues were prepared as previously described [28] and Western blot assays were conducted as reported earlier [10,11]. Bands were visualized by the enhanced chemiluminescence detection system (Amersham Pharmacia, Little Chalfont, United Kingdom) according to the manufacturer's instructions.

Primary Antibodies

A panel of different anti-CTCF antibodies with different characteristics was used: rabbit polyclonal [Abcam (Cambridge, United Kingdom) and Millipore (Billerica, MA)] , mouse monoclonal (BD Biosciences, Oxford, United Kingdom), and the mixture of nine anti-CTCF monoclonal antibodies [10,29,30]. The use of these antibodies in specific experiments is described in the figure legends. Other antibodies were given as follows: mouse monoclonal anti–α-tubulin (Sigma-Aldrich, St Louis, MO); RNA Polymerase II (N-20), SP1, WT1, EGR1, and c-Myc [all rabbit polyclonal from Santa Cruz Biotechnology (Santa Cruz, CA)]; mouse monoclonal me3H3K4 and me3H3K27 (Millipore); rabbit polyclonal PARP-1 (Enzo, Exeter, United Kingdom); mouse monoclonal H3K9Ac and me3H3K9 (Diagenode, Liège, Belgium); rabbit polyclonal His-Tag and Bax (Cell Signaling Technology, Danvers, MA). The staining protocols are available on request.

CTCF and Terminal Deoxynucleotidyl Transferase–Mediated Deoxyuridine Triphosphate Nick End Labeling Staining

For CTCF immunostaining, cells were fixed with 4% paraformaldehyde, permeabilized with 0.2% Triton X-100 in 1× phosphate-buffered saline (PBS), blocked with 1% normal goat serum in 1× PBS, and incubated with the anti-CTCF rabbit polyclonal antibody (Abcam) and then with the fluorescein isothiocyanate (FITC)–labeled anti-rabbit IgG (Dako, Ely, United Kingdom). To detect cells undergoing apoptosis, cells were stained by terminal deoxynucleotidyl transferase–mediated deoxyuridine triphosphate nick end labeling (TUNEL), using *In Situ* Cell Detection Kit, TMR red (Roche Applied Science, West Sussex, United Kingdom) following the manufacturer's instructions. Nuclei were stained with 4,6-diamidino-2-phenylindole dilactate (DAPI; Sigma-Aldrich) at 5 μg/ml. Images were taken using Bio-Rad Laboratories (Hercules, CA) confocal or BX-41 (Olympus, Southend-on-Sea, United Kingdom) microscopes. Images were analyzed with ImageJ software [31]. The values were measured for CTCF and TUNEL staining. The mean values for fluorescence were normalized by subtracting the background values and presented as scatter plots.

Purification of RNA, Reverse Transcription, and Real-Time Reverse Transcription–Quantitative Polymerase Chain Reaction

Total RNA was isolated with Trisure (Bioline, London, United Kingdom) as described by the manufacturer. RNA was treated with TURBO DNA-free kit (Ambion, Paisley, United Kingdom); 1 μg

of total RNA was used for reverse transcription (RT) with VERSO cDNA kit (Thermo Fisher, Loughborough, United Kingdom). For RT–quantitative polymerase chain reaction (qPCR), cDNA samples were diluted at 1:10. A 25-μl PCR mix consisted of 1× SensiMix Plus SYBR (Quantace, London, United Kingdom), 2 μl of diluted cDNA, 200 nM of each primer, and 3 mM $MgCl_2$. Amplification, data acquisition, and analysis were carried out using the Chromo4 Real-Time PCR (Bio-Rad Laboratories). The comparative C_t method was used to assess relative changes in *mRNA* levels [32]; calculations were made according to Pfaffl [32]. Primers and conditions for RT-qPCR are described in the Supplemental Materials and Methods section.

Chromatin Immunoprecipitation Assays

Chromatin immunoprecipitation (ChIP) assays were performed from cross-linked cells (~1×10^6) or fresh tissues (50–100 mg) using Protein A agarose/salmon sperm DNA beads (Millipore) or Protein A-BioVyon Gravity free flow columns (Porvair Technology, Wrexham, United Kingdom) as described previously [33]. For experiments, tissues were finely diced in 10 ml of Leibovitz's L-15 media, cross-linked with 1% of formaldehyde, and quenched for 5 minutes with glycine (0.125 M final). The suspension was centrifuged at 1500 rpm for 3 minutes, pellet resuspended in ice-cold PBS, homogenized using the Polytron Homogenizer, and passed through a syringe to achieve a single cell suspension. Following centrifugation, the cell pellet was collected and processed for ChIP as for cell lines [33]. Immunoprecipitated DNA was extracted with phenol/chloroform and ethanol precipitated. Real-time PCR was carried out in triplicate using 2 μl of the immunoprecipitated DNA sample and input DNA and 300 nM primers diluted to a final volume of 25 μl in SensiMix Plus SYBR (Quantace). Percentage of DNA brought down by ChIP (% input) was calculated as follows: input = AE^(Ctinput − CtChIP) × Fd × 100% (AE is amplification efficiency, CtChIP and CtInput are threshold values obtained from exponential phase of qPCR, and Fd is a dilution factor of the input DNA to balance the difference in amounts of ChIP). Primers and conditions for qPCR are available in the Supplemental Materials and Methods section.

Electrophoretic mobility shift assays (EMSAs) were performed as previously described [30,34]. In brief, eight consecutive overlapping fragments, ~200 bp in length, covering the *Bax* gene promoter from position −600 to +550 relative to the +1 transcription start site [19] were generated by PCR. Primers and conditions for PCR are available on request. Fragments were then end-labeled using ^{32}P-γ-ATP and T4 polynucleotide kinase, incubated with the *in vitro* translated CTCF (ZF domain or full length), and resolved on 5% non-denaturing polyacrylamide gels. The correct sizes of the *in vitro* translated CTCF ZF domain and the full-length CTCF protein were confirmed by gel electrophoresis in 8% sodium dodecyl sulfate–polyacrylamide gel electrophoresis (SDS-PAGE), in combination with Western blot analysis (data not shown).

The Bax *Gene Promoter Constructs for Luciferase Reporter Assays*

The *Bax* promoter region was amplified from human genomic DNA purified from white blood cell using the following primers: (forward) 5′-ggttatctcttgggctcacaag-3′ and (reverse) 5′-tgatggacgggtccggggagca-3′. The fragment was subcloned into the pDrive vector (Qiagen), verified by sequencing, and then cloned into the multiple cloning sites (*Kpn*I and *Hin*dIII) of the promoter-less pGL2-Basic vector (Promega, Southampton, United Kingdom).

Cell Transfection and Luciferase Assay

HeLa, 293T, and Cama1 cells (all seeded at 1.2×10^5) and MCF-7 (2.5×10^5) were transiently transfected with 5 μg of total DNA (3 μg of reporter plasmid, 1 μg of pCi or pCiCTCF, and 1 μg of carrier DNA) using calcium phosphate method as previously described [11]. pCiCTCF is a vector based on pCi plasmid (Promega) expressing His-tagged human CTCF protein [29]. Transfected cells were harvested 48 hours post-transfection. Luciferase was measured with the Luciferase Assay System (Promega) following the manufacturer's instructions and calculated in relative light units after normalization against β-galactosidase activity or percentage of pEGFP-positive cells, used as controls for transfection efficiency.

Cell Survival Assay

Cell survival (viability) was measured using microculture tetrazolium test (MTT) from (Sigma-Aldrich) as described in the manufacturer's manual. Briefly, 20 μl of 5 mg/ml MTT was added to the wells and cells were incubated at 37°C for 3.5 hours. The medium was then removed, and 150 μl of the MTT solution was added to the cells for further incubation for 15 minutes at room temperature with shaking. The OD_{590} and OD_{620} were read using Versamax plate reader. Control cells were treated with DMSO (0.1%) or water alone. Cell survival was calculated as a percent of control (DMSO-treated in experiments with Taxol or water-treated in experiments with Mitoxantrone) cells as described previously [35].

Statistical Analysis

Statistical analysis was carried out using unpaired Student *t* test. A significant value was detected when the probability was below the 5% confidence level ($P < .05$).

Results

Knockdown of CTCF with siRNA Leads to Apoptotic Cell Death in Breast Cancer Cells

In this study, we first aimed to reproduce the anti-apoptotic effects of CTCF in breast cancer cells using siRNA, a more efficient tool than the previously employed antisense RNA [11]. The efficient knockdown of CTCF (referred as CTCF-130 because it migrates as a 130-kDa protein) was achieved by the Hs_CTCF_4 siRNA in breast cancer cells, ZR75.1, and led to apoptosis (Figure 1*A*). These results were verified by immunofluorescence analysis of transfected cells, whereby only TUNEL-positive apoptotic cells contained significantly lower levels of CTCF (Figure 1*C*). Similar results were obtained using another breast cancer cell line, MCF-7 (Figure W1, *A* and *B*). No significant effects on cell viability and apoptosis from the Hs_CTCF_4 siRNA were observed in non–breast cancer cell lines (Figure 1, *B* and *C*, and data not shown). Other commercially available CTCF siRNAs (Hs_CTCF_1 through Hs_CTCF_3 siRNA and CTCF SMARTpool siRNA) were also able to efficiently knock down CTCF and reproduce the specific apoptotic effects observed with the Hs_CTCF_4 siRNA in breast cancer cells (Figure W2 and data not shown). Correlation between the lower intensity of CTCF staining with higher intensity of TUNEL staining was further confirmed using unbiased quantification of the images of breast and non–breast cells with depleted levels of CTCF (Figures 1*C* and W1*C*). Of note, using the same experimental conditions, the control siRNA successfully targeted the corresponding *cyclophilin B* mRNA in four cell lines following transfection with the *cyclophilin B* siRNA (Figure W3). Treatment with the *cyclophilin B* siRNA did not have any visible biologic effects on the cells (data not shown).

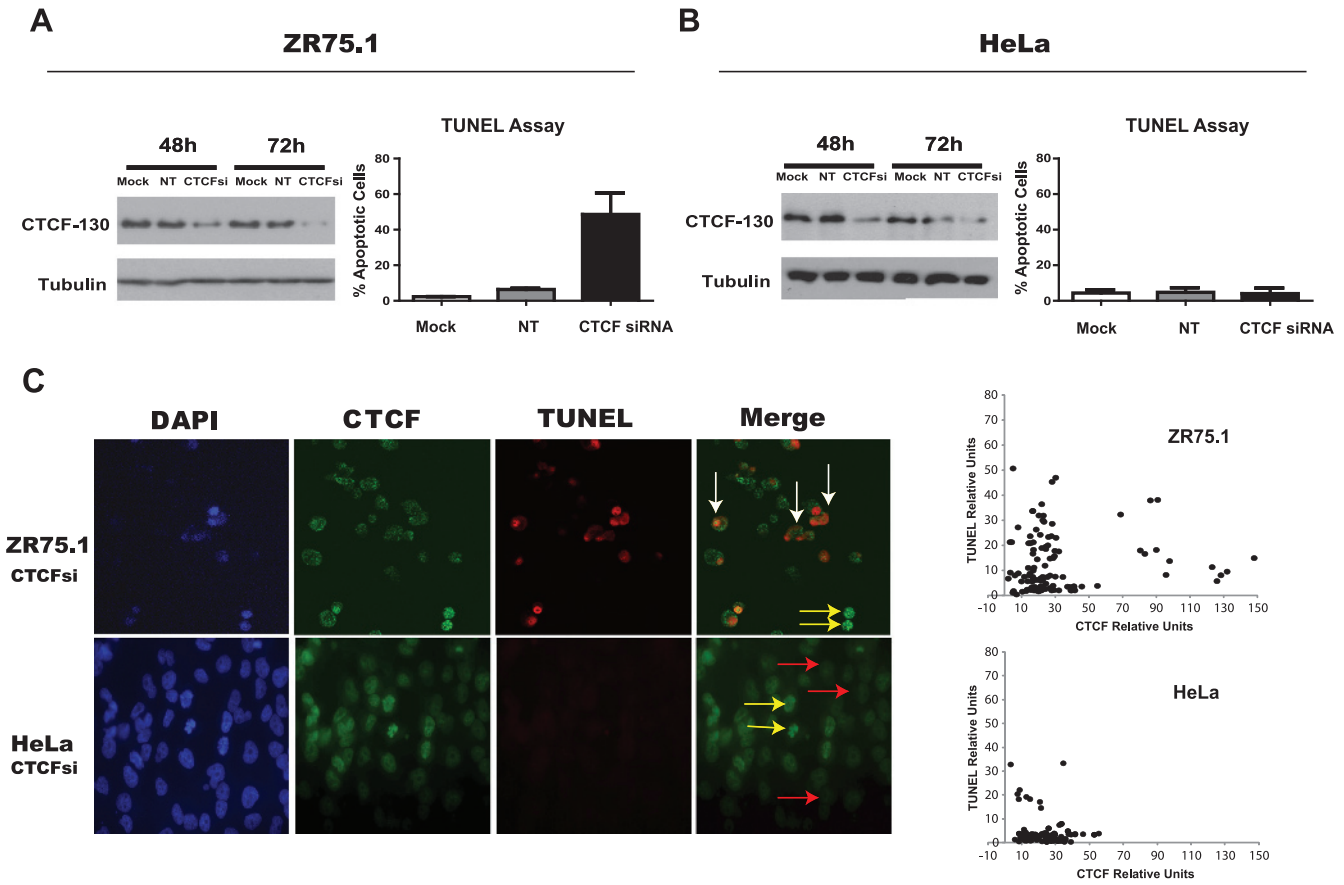

Figure 1. Transient CTCF knockdown by CTCF siRNA induces specific apoptotic cell death in breast cancer cells. (A and B) Left: Levels of CTCF are reduced in breast cancer (ZR75.1) and cervical carcinoma (HeLa) cells treated with the Hs_CTCF_4 siRNA as shown by Western blot analysis. ZR75.1 (2.5×10^5) and HeLa (1.2×10^5) cells were transfected with 50 pM target siRNA (CTCF siRNA, "CTCFsi") and non-target siRNA ("NT") or transfection reagent only ("Mock"). Forty-eight and 72 hours post-transfection, cells were collected, cellular extracts were prepared, and equal amounts (40 μg) of total protein were loaded onto SDS-PAGE. Samples were electrophoretically separated, blotted, and probed with the mouse monoclonal anti-CTCF antibody (BD Biosciences). The membrane was reprobed with the anti–α-tubulin antibody, which served as an internal control for protein loading. "CTCF-130" refers to CTCF migrating as 130-kDa protein. Right: Apoptotic cell death is induced following CTCF knockdown with the CTCF siRNA in ZR75.1 (A) but not in HeLa (B) cells. ZR75.1 (2.5×10^5) and HeLa (1.2×10^5) cells were transfected with 50 pM target siRNA (CTCF siRNA, "CTCFsi") and non-target siRNA ("NT") or transfection reagent only ("Mock"); apoptotic cell death was assessed by TUNEL assay. The percentage of TUNEL-positive cells was calculated 48 hours after transfection. The results represent the mean values with the SDs (error bars) of three independent experiments. (C) Reduced CTCF levels are associated with apoptosis in ZR75.1 cells (upper panel) but not in HeLa cells (lower panel). ZR75.1 and HeLa cells were transfected with CTCF siRNA as above and analyzed by immunofluorescence staining with the rabbit polyclonal anti-CTCF antibody (Abcam; FITC, green fluorescence). Apoptotic death was assessed by TUNEL staining (TMR, red fluorescence). Nuclei were visualized by DAPI. Merge, overlay of CTCF and TUNEL staining. ZR75.1 breast cancer cells with low levels of CTCF are apoptotic (TUNEL-positive), as indicated by white arrows, whereas HeLa cells with low levels of CTCF remain TUNEL-negative (red arrows). Cells with high levels of CTCF (not transfected with CTCF siRNA) are TUNEL-negative (yellow arrows). Images were additionally analyzed using the ImageJ software [31]. The values were measured for CTCF and TUNEL staining in 100 cells; the mean values for fluorescence were normalized by subtracting the background values. The results obtained in ZR75.1 and HeLa cells are presented as scatter plots on the right.

We concluded that CTCF levels can be specifically downregulated using different anti–CTCF siRNAs. The Hs_CTCF_4 siRNA was selected for all subsequent experiments in this report and referred to as CTCF siRNA.

Levels of the Endogenous Bax *mRNA and Protein Increase in Breast Cancer Cells Following CTCF Knockdown*

Our previous data demonstrated that the levels of Bax protein in breast cancer cells are increased following CTCF knockdown by antisense RNA [11]. To investigate whether CTCF regulates the *Bax* gene at the transcriptional level, we studied *Bax* mRNA in representative breast (ZR75.1 and MCF-7) and non–breast (HeLa and 293T) cells, 24 and 48 hours post-transfection with CTCF siRNA. Efficient inhibition of *CTCF* mRNA was observed in all cells at both time points, whereas effects in cells transfected with controls, i.e., non-target siRNA and the reagent only ("Mock"), were insignificant (Figure 2*A*). Following CTCF depletion, the levels of *Bax* mRNA increased modestly, but significantly, in breast cancer cells, compared with cells transfected with non-target siRNA and "mock" transfected. In contrast, no significant changes in *Bax* mRNA were detected in non–breast cells (Figure 2*B*). Levels of *Bax* mRNA in breast cancer cells also increased following CTCF knockdown by a different CTCF siRNA (the CTCF SMARTpool siRNA; Figure W4*A*). In parallel with the mRNA, the amounts of Bax protein also increased in breast cancer cells after CTCF depletion (Figures 2*C* and W4*B*). Elevation of Bax in these cells was

accompanied by the generation of the 89-kDa fragment (hallmark of apoptosis) resulting from the cleavage of PARP-1 (116 kDa; Figure 2*C*) [36,37]. The apoptotic events are likely to be mainly driven by Bax overexpression because the levels of the cleaved 89-kDa fragment were considerably decreased in cells with double knockdown of CTCF and Bax (Figure 2*D*, *left panel*). Furthermore, the assessment of cell viability of these cells in the MTT assay revealed significantly more viable cells in the double knockdown experiments than in those where cells were transfected with the CTCF siRNA (Figure 2*D*, *right panel*).

CTCF Protein Binds to Two Sites within the Promoter-Proximal Region of Human Bax *Gene*

We hypothesized that CTCF may regulate transcription of the *Bax* gene in breast cancer cells by interacting with its promoter. To identify the regions bound by CTCF, we used EMSA with a series of fragments overlapping the promoter region of *Bax* (Figure 3*A*). The DNA binding domain of CTCF (ZF) formed retarded complexes with the known site Myc A [34] and *Bax* fragments 5 and 6 (Figure 3*B*, *red arrows*); the latter was further confirmed using the full-length *in vitro* translated CTCF (Figure W5). A retarded complex was also observed between the ZF domain and fragment 7 (Figure 3*B*, *blue arrow*); however, the DNase I footprinting analysis later revealed that the overlapping fragments 6 and 7 share the common CTCF binding site, CTS-2 (see text below and Figure 3*C*). Indeed, no DNA-protein complexes were detected when a shorter fragment (fragment 8), which lacks CTS-2, was used in EMSA (Figure 3*B*).

In vitro DNase I footprinting assay was used to determine more precisely the locations of the CTSs within fragments 5 and 6 (Figure W6*A*).

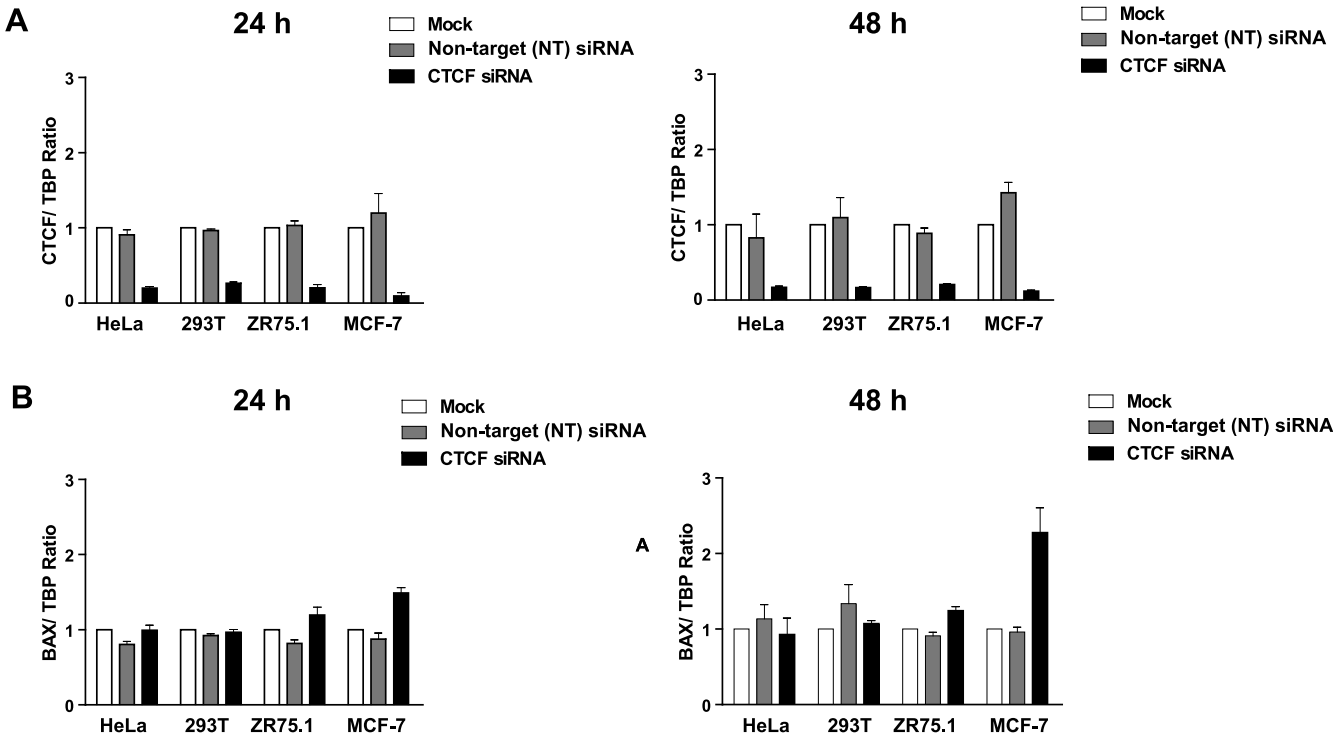

Figure 2. Increased levels of *Bax* mRNA and protein after CTCF knockdown in breast cancer cells are associated with the hallmarks of apoptosis. (A and B) Levels of *Bax* mRNA increase in breast cancer cells following CTCF knockdown. Non–breast cells HeLa (1.2×10^5) and 293T (1.2×10^5) and breast cancer cells ZR75.1 (2.5×10^5) and MCF-7 (2.5×10^5) were transfected with 50 pM CTCF siRNA, non-target siRNA, or transfection reagent only ("Mock") and harvested 24 and 48 hours post-transfection. Total RNA was prepared and analyzed by RT-qPCR. The expression levels of *CTCF* (2A) and *Bax* mRNA (2B) were calculated using the comparative C_t method ($\Delta\Delta C_t$) and normalized to *TBP* mRNA expression. Columns represent fold change of *CTCF/TBP* mRNA or *Bax/TBP* mRNA levels relative to mock-transfected cells (designated as 1.0) as shown in the diagrams. For each sample, measurements were done at least in triplicates; error bars represent SDs. The difference in both *CTCF* and *Bax* mRNA levels between cells treated with CTCF siRNA and control (non-target, NT) siRNA was statistically significant ($P \leq 0.01$). (C) Levels of Bax protein increase and the apoptotic markers appear in breast cancer cells following CTCF knockdown. Non–breast and breast cancer cells were transfected as described above, collected 24 and 48 hours post-transfection, lysed, proteins separated by SDS-PAGE, transferred onto a membrane, and analyzed by Western blot analysis to assess the levels of CTCF, Bax, and PARP-1 (full size, 116 kDa and the cleavage fragment, 89 kDa). Asterisks indicate the samples treated with the CTCF siRNA, and arrows indicate the position of the PARP-1 cleavage fragment. (D) Apoptosis is considerably less pronounced in cells double transfected with CTCF siRNA and Bax siRNA than in cells transfected with CTCF siRNA only. MCF-7 and ZR75.1 cells were transfected with 50 pM CTCF siRNA or Bax siRNA, combination of CTCF and Bax siRNA (50 pM each), 50 pM non-target siRNA, or transfection reagent only ("Mock") and analyzed by Western blot analysis as described above. The results are shown in panels on the left. Arrows indicate the position of the PARP-1 cleavage fragment. For the MTT assay (graphs on the right), cells were prepared as described above, treated with trypsin (24 hours post-transfection), counted, replated onto 96-well plates at 5×10^4 per well, and incubated overnight. After a total of 48 hours post-transfection, the medium was changed to the phenol-free RPMI. Cell survival was measured using MTT assay as described under Materials and Methods section. The results represent the mean values with the SDs (error bars) of three independent experiments. Abbreviations for C and D: CTCFsi, CTCF siRNA; NT, non-target siRNA; Baxsi, Bax siRNA; M, transfection reagent only ("Mock"); C, control (extracts from untreated cells).

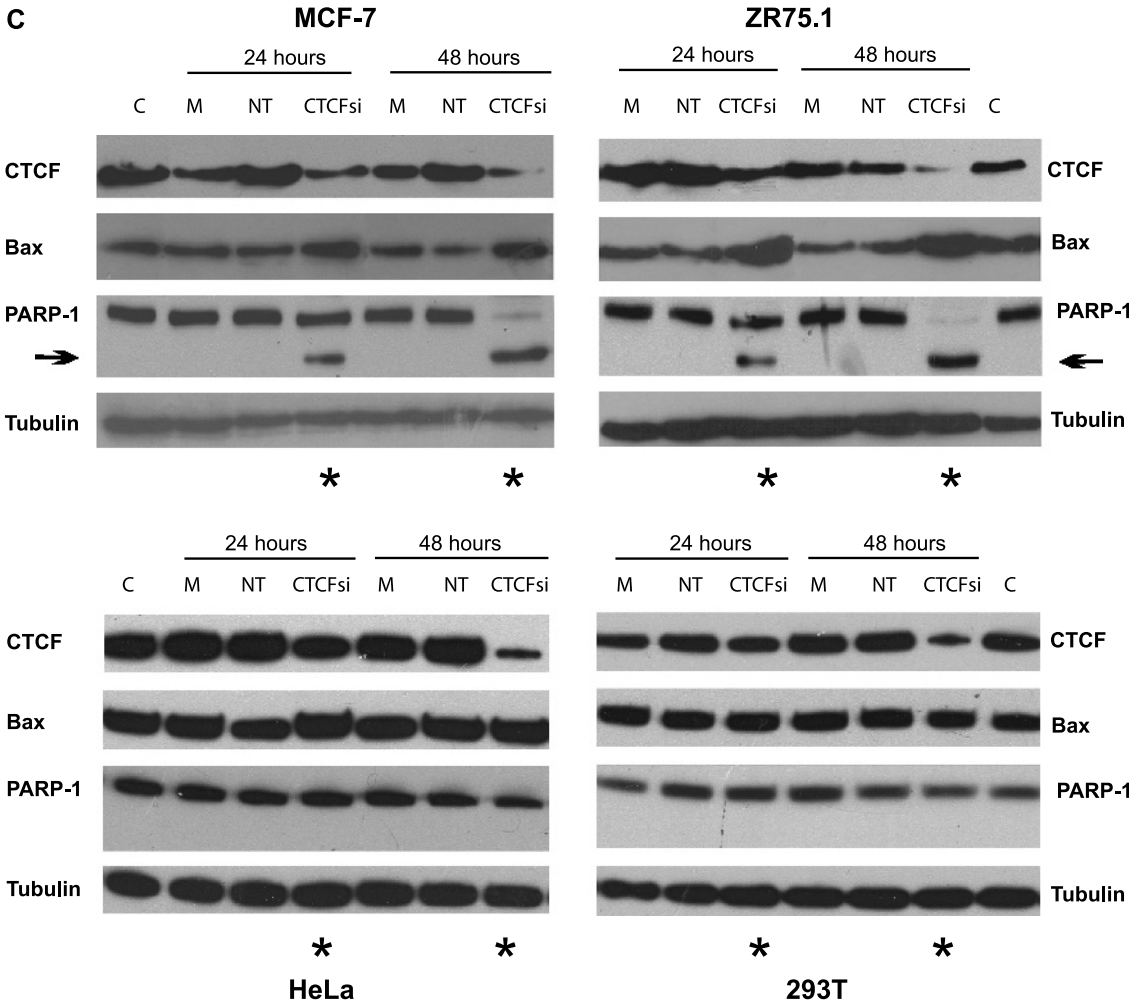

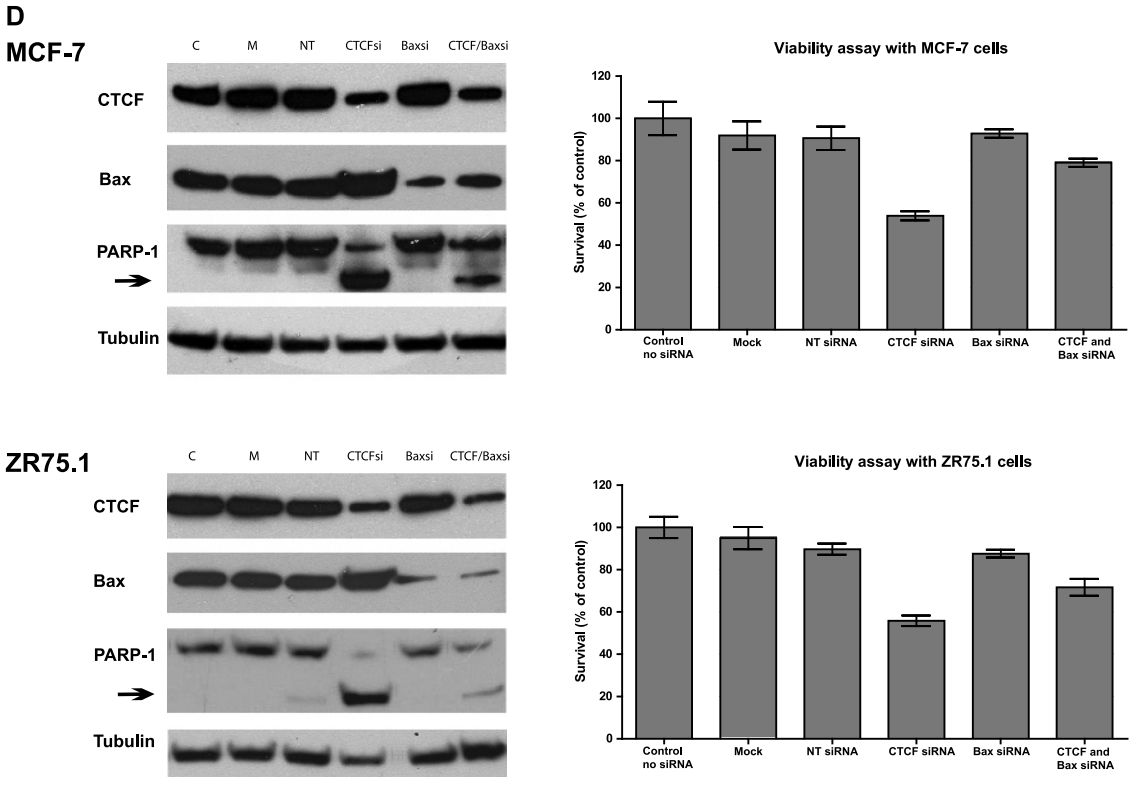

Figure 2. (*continued*).

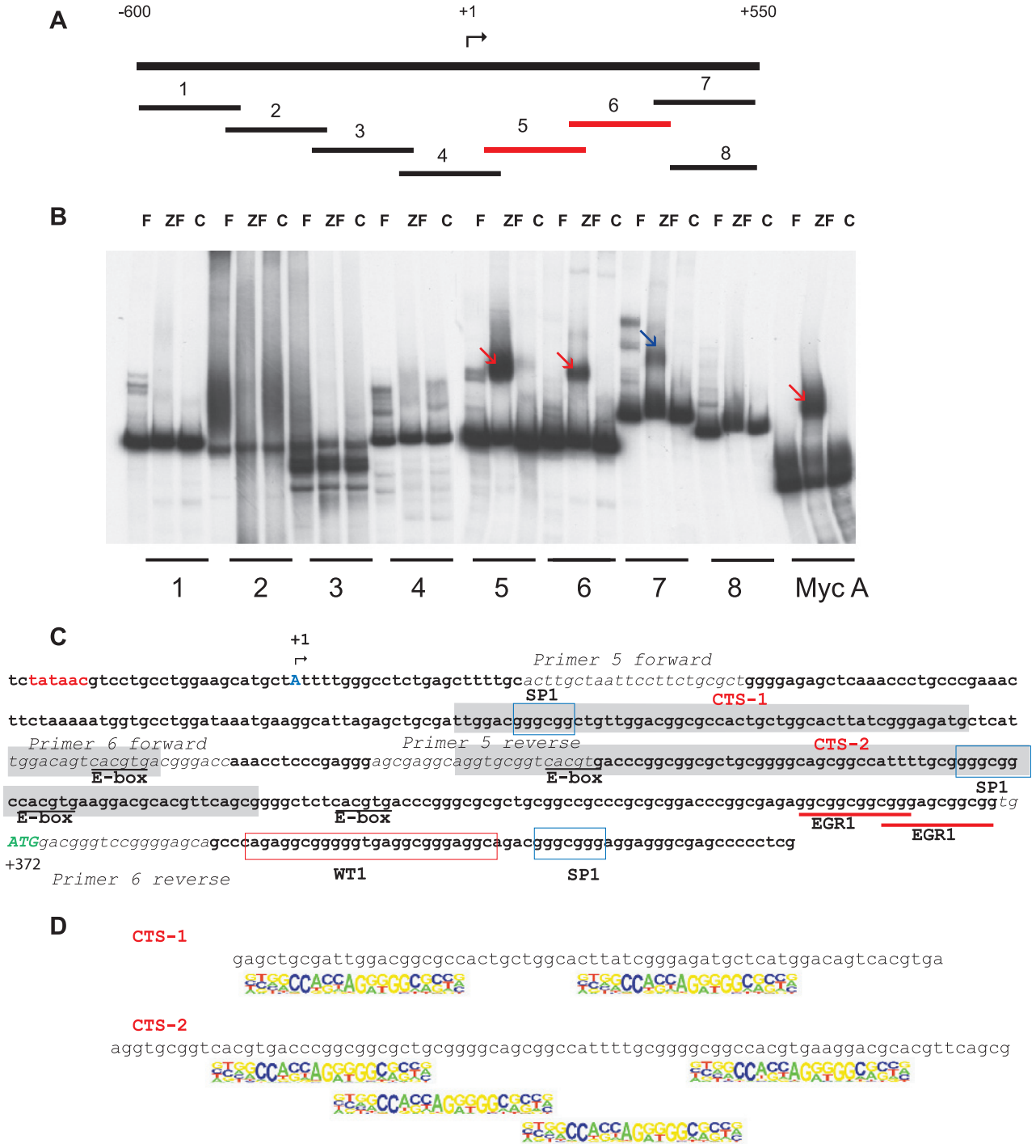

Figure 3. CTCF binds to two sites within the promoter-proximal region of human *Bax* gene in the EMSA. (A) A schematic representation of the approach to identify CTSs in the promoter region of the human *Bax* gene. The eight overlapping fragments, generated by PCR, each of approximately 200 bp in length, are positioned within the 1150-bp promoter region of the human *Bax* gene. The transcription start site identified previously [19] is indicated as +1. Fragments 5 and 6 positive for CTCF binding are depicted in red. (B) EMSA analysis of CTCF binding to the overlapping fragments of the human *Bax* promoter. The DNA fragments shown in A were end-labeled with ^{32}P, and EMSA analyses were performed as described under Materials and Methods section. The *in vitro* translated 11-Zn-finger domain of CTCF (ZF) and luciferase (control, C) were used to assess specific and non-specific binding to the DNA, respectively. F, free probe. A DNA fragment from the human *c-Myc* promoter containing the CTS A (Myc A) [34] served as a positive control for CTCF binding. Specific DNA complexes with the ZF domain of CTCF and fragments 5 and 6 are indicated by red arrows and fragment 7 by the blue arrow. (C) Nucleotide sequence of the region of the human *Bax* gene promoter comprising CTSs. The previously identified transcription start site [19] is indicated (+1, blue capital letter A). TATA box is shown in red, and the translation start site (ATG, +372) is depicted in green capital letters. Two sequences, CTS-1 and CTS-2, protected by CTCF from DNAse I are highlighted in gray. The forward and reverse primers used to generate fragments 5 and 6 are shown in italic. The E-box elements (potential sites for c-Myc binding) are underlined. Consensus binding sites for SP1 and WT are boxed in blue and red, respectively. EGR1 binding sites are underlined with red lines. (D) The regions within *Bax* fragments 5 and 6 protected by CTCF (named CTCF-1 and CTCF-2, respectively) contain sequences that comply with the CTCF motif identified by Kim et al. [42].

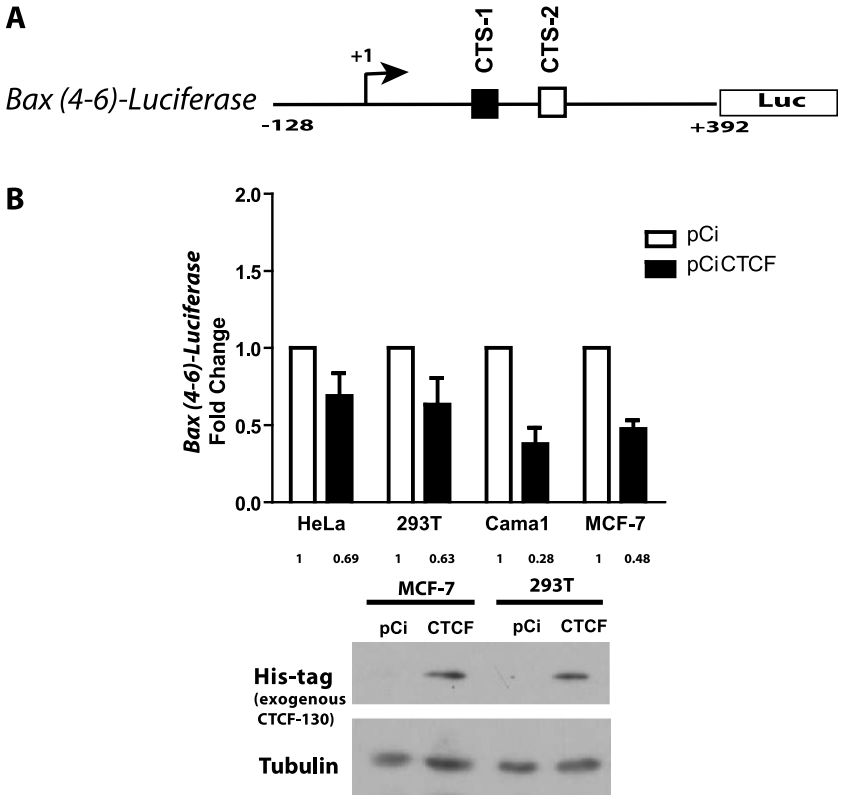

Figure 4. The *Bax*-luciferase reporter construct, containing CTSs, is negatively regulated by CTCF. (A) Cartoon illustration of the luciferase-based reporter construct driven by the fragment of the human *Bax* gene promoter containing the two CTSs. Position of the transcription start site (+1) is indicated. Both CTSs are shown as white and black boxes. (B) CTCF overexpression results in down-regulation of the reporter. Cells were transiently transfected with the reporter construct and pCiCTCF [29] and the empty control plasmid pCi, harvested, and assayed for luciferase activity as described in Materials and Methods section. Bars represent fold changes of luciferase activity in the cells transfected with the plasmid expressing CTCF (pCiCTCF) [29] compared with the controls, mock-transfected or transfected with the empty vector pCi, respectively (taken as 1); the numerical values are shown under each column. The mean of three independent experiments is shown. Error bars indicate SDs. The difference in luciferase values between cells transfected with pCiCTCF and the corresponding control (pCi) were statistically significant ($P < .05$). The levels of the exogenous, His-tagged CTCF were assessed by Western blot assay using the anti–His-Tag antibody, respectively; these results are shown below the graphs. The membrane was reprobed with an anti-tubulin antibody (loading control). "CTCF" refers to the exogenous CTCF produced from pCiCTCF; pCi is an empty vector.

The first CTS (CTS-1) spans the region between +117 and +185, and the second (CTS-2) spans the region between +216 and +296, downstream of the transcription start site (Figure W6*B*). These results are summarized schematically in Figure 3*C*. Notably, in both fragments, the protected DNA sequences are long, which is a usual requirement to form a complex with CTCF [38–40]. Moreover, each fragment contains several sequences that match the CTCF "consensus" motif [41–44] (Figure 3*D*). Analysis of the ChIP-seq data of CTCF binding in MCF-7 cells deposited in the UCSC genome browser revealed the enrichment for CTCF binding in this region, thus supporting further our experimental findings (Figure W6, *C* and *D*).

It was previously noted that CTSs positioned downstream of transcriptional start sites, for example, in the *c-MYC* and *hTERT* genes, are likely to act as repressors [34,45]. Our observations that CTCF knockdown leads to up-regulation of Bax ([11] and this study), together with two potential CTSs located downstream from the transcription start in the promoter of the *Bax* gene (Figure 3*C*), suggested that CTCF negatively regulates *Bax* transcription. To test this hypothesis, we generated a luciferase reporter plasmid based on the promoter-less pGL2, driven by the 520-bp fragment of the *Bax* gene promoter encompassing fragments 5 and 6 (Figure 4*A*) and measured the luciferase activity following CTCF overexpression. In these experiments, CTCF overexpression led to significant down-regulation of the reporter. The efficient production of the ectopic His-tagged CTCF was confirmed by Western blot analysis (Figure 4*B*).

The Active State of the Bax *Gene in Breast and Non–Breast Cancer Cells Is Associated with Open Chromatin Configuration and Unmethylation of the* Bax *Gene Promoter Harboring the CTSs*

To investigate the molecular mechanisms of the specific anti-apoptotic function of CTCF in breast cancer cells, we first compared the levels of *Bax* mRNA and protein in a number of cell lines. *Bax* was expressed in all cases, with no significant difference in *Bax* mRNA and protein levels between breast and non–breast cells (Figure 5*A*). *Bax* expression was associated with open chromatin marks (Figure 5*B*) and the presence of the RNA Polymerase II at the *Bax* DNA fragments containing the CTSs (Figure 5*B*) and the TATA box (Figure 5*C*).

These findings are further supported by the data from the UCSC genome browser showing the presence of marks associated with active transcription, in the CTSs within the *Bax* promoter, in a variety of breast and non–breast cancer cells (Figure W7).

We next tested if the differential binding of CTCF to the *Bax* promoter was methylation dependent using the bisulfite sequencing strategy. We found that the CTCF binding regions of the *Bax* promoter were unmethylated in all the cell lines (breast and non-breast) and

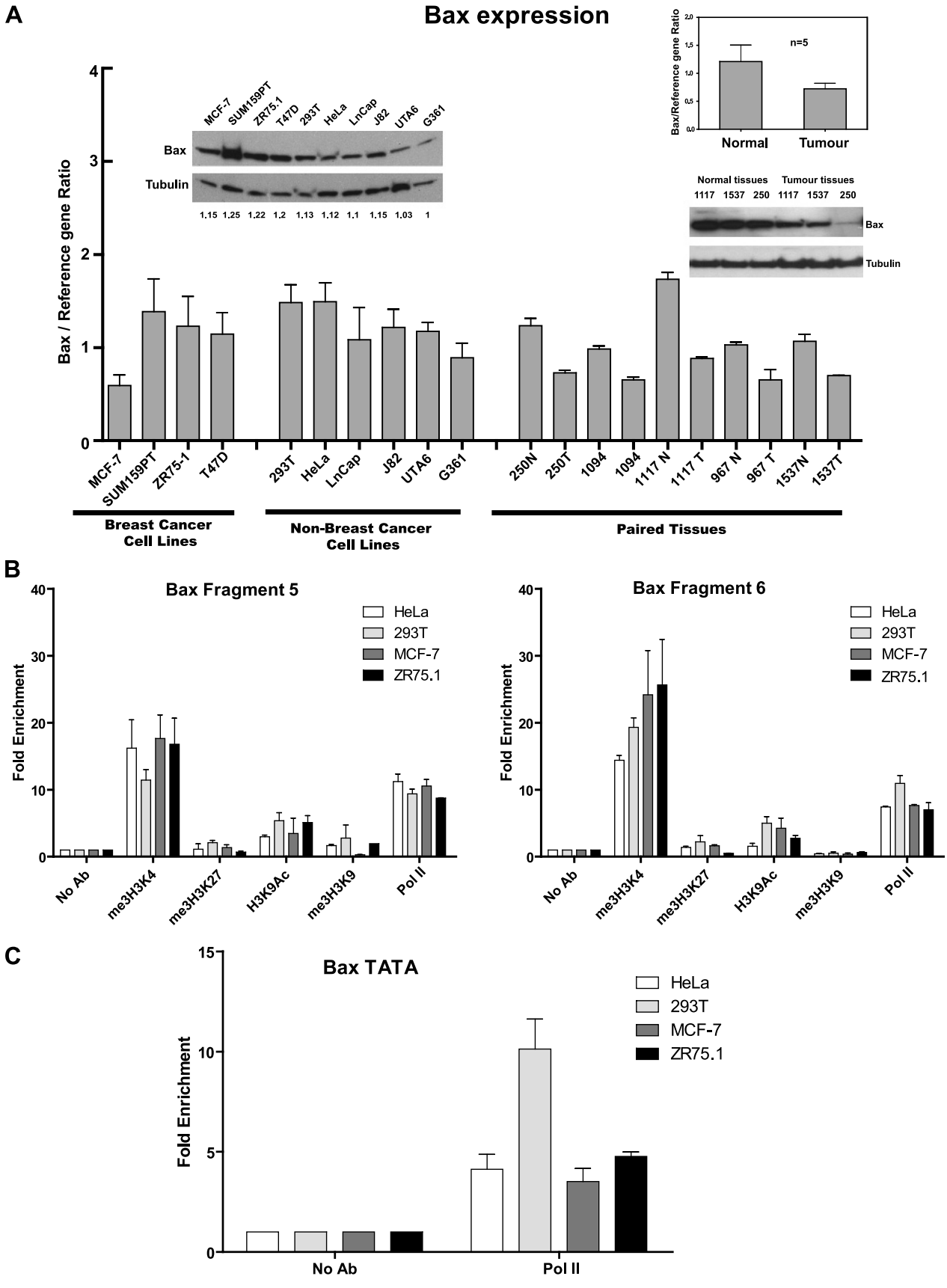

breast tissues (normal and tumor) analyzed (Figure W8). Therefore, different epigenetic mechanism(s) may be in operation to provide differential regulation of *Bax* in breast and non–breast cells.

The CTSs Are Enriched with CTCF in Breast Cancer Cells Compared with Normal Breast and Non–Breast Cancer Cells

We proposed that the specific apoptotic phenotype in CTCF-depleted breast cancer cells may be explained by the increased CTCF binding to the *Bax* promoter in breast compared with the non–breast cells. To explore this possibility, we investigated the *in vivo* occupancy by CTCF of fragments 5 and 6, harboring CTS-1 and CTS-2, respectively, in breast and non–breast cell lines using ChIP assay [30,42]. As shown in Figure 6*A*, considerable enrichment of CTCF binding to both fragments was observed in the two breast cancer cell lines inspected. In contrast, in non–breast cell lines, CTCF binding to either of these fragments was reduced.

We then asked whether the CTSs in non–breast cells may be enriched with other transcription factors than CTCF. Bioinformatics (MatInspector, www.genomatrix.de) and literature analyses were used to identify transcription factors that could potentially bind to the *Bax* promoter region containing CTSs. Four such factors were selected on the basis of the published data and high score matches: WT1 [16], EGR1 [17], c-Myc [18], and SP1 (their positions are indicated in Figure 3*C*). ChIP experiments revealed no significant differences in the enrichment of fragment 5 (CTS-1) by SP1, WT1, and EGR1, whereas the enrichment by c-Myc was higher in non–breast cells (Figure 6*B*, *left*). In contrast, the occupancy of fragment 6 (CTS-2) by all factors was significantly lower in breast cells than in non–breast cells (Figure 6*B*, *right*). These observations suggest differential functions of the two CTSs. This line of investigation was not pursued in this study because of close proximity of the CTSs; further evidence will be required to corroborate this finding.

We then investigated the link between *Bax* mRNA expression and the CTS occupancy by CTCF and other factors in breast tumors and paired peripheral (referred here as "normal") tissues. Consistent with published data [46], *Bax* mRNA was found to be expressed at higher levels in normal tissues compared with the corresponding paired tumors and this was also observed with the levels of Bax protein (Figure 5*A*). Moreover, enrichment of CTCF binding to both Bax fragments 5 and 6 was detected in tumor tissues, compared with normal breast tissues (Figures 6*C* and W9, and data not shown). To study the occupancy of these fragments by other factors, the paired tissue specimens 1094, which provided sufficient material to perform multiple ChIP assays, were used. As shown in Figure 6*C*, similar to CTCF, WT1 was enriched in the tumor tissue, whereas binding of SP1, EGR1, and c-Myc was higher in the normal tissue.

We then asked whether the levels of the Bax protein and the binding of CTCF to the CTSs would be the same or different in a non–breast cell line stably overexpressing ectopic CTCF. For this purpose, we used leukemia cells K562-G1 previously generated and characterized in our laboratory [26]. As shown in Figure 7*A*, K562-G1 cells produce considerably more CTCF protein than control cells (original K562 unmodified cell line and K562EV stably transfected with the backbone empty plasmid pcDNA3), whereas no change in Bax levels can be observed. There was no difference in CTCF binding to fragments 5 and 6, and the occupancies of these fragments by WT1, SP1, EGR1, and c-Myc were also generally similar in the three cell lines (Figure 7*B*). Reduction of CTCF levels in the original K562 and K562-G1 cells led to increased proliferation and inhibition of erythroid differentiation but had no effect on apoptotic cell death ([26] and data not shown).

From these results, we conclude that in breast cancer cells (tissues and cell lines) CTCF binding to the *Bax* promoter proximal regions is increased, compared with non–breast cells and normal breast tissues where other transcription factors are predominantly bound.

Discussion

In this report, we present experimental evidence for the transcriptional regulation of the pro-apoptotic gene *Bax* by CTCF in breast cancer cells. Using specific CTCF siRNA, we confirmed our previous observations that knockdown of CTCF leads to apoptosis specifically in breast cancer cells but not in non–breast cancer cells. This study clarified the link between CTCF and Bax, whereby depletion of CTCF led to the increase in levels of *Bax* mRNA and protein in breast cancer cells but not in non–breast cancer cells. Although the changes in *Bax* mRNA expression were modest, they were sufficient to induce apoptosis; similar observations were described in another report [47]. It

Figure 5. The active state of the *Bax* gene in different cell lines and tissues is associated with open chromatin hallmarks. (A) Analysis of *Bax* mRNA and protein levels in breast and non–breast cell lines and in normal and tumor breast tissues. Total RNAs were prepared and analyzed by RT-qPCR as described under Materials and Methods section. The expression levels of *Bax* mRNA were calculated using the comparative C_t method ($\Delta\Delta C_t$) and normalized to *TBP* mRNA expression. For each sample, measurements were done at least in triplicates. The comparison between the mean *Bax* mRNA levels in normal and tumor tissues ($n = 5$) is shown in the inserted diagram. Error bars represent SDs. Western blot analyses of different cell lines (left) and selected tissue samples (right) are represented by the images inserted above bars. Cellular or tissue extracts (20 μg of total protein) were loaded onto SDS-PAGE, separated, blotted, and probed with the anti-Bax antibody. The same membrane was stripped and reprobed with the α-tubulin antibody (loading control). For cell samples, the developed films were scanned using the ImageJ software and images were quantified. The ratios of the intensity of the Bax bands over the intensity of the corresponding α-tubulin bands were determined and expressed as fold change relative to the lowest Bax/α-tubulin ratio (designated as 1.0). Numbers below each lane represent these results. (B) Open chromatin marks and RNA Polymerase II are present at the *Bax* CTSs. Non–breast and breast cells (~1×10^6) were prepared for ChIP and immunoprecipitated with the antibodies for repressive (me3H3K27 and me3H3K9) and active (me3H3K4 and H3K9Ac) chromatin and RNA Polymerase II (Pol II). DNA was extracted and qPCR was performed using primers specific to *Bax* fragments 5 and 6. Results were calculated as the percentage of input chromatin precipitated at the region of interest and presented as fold change relative to the control ChIP experiment with no antibody (designated as 1.0; see Materials and Methods section for details). Experiments were performed in triplicate and the mean value is shown. Error bars indicate SDs. (C) RNA Polymerase II is present at the TATA box of *Bax* gene. The ChIP experiments were conducted as described in B; primers overlapping the TATA box *Bax* gene were used for qPCR.

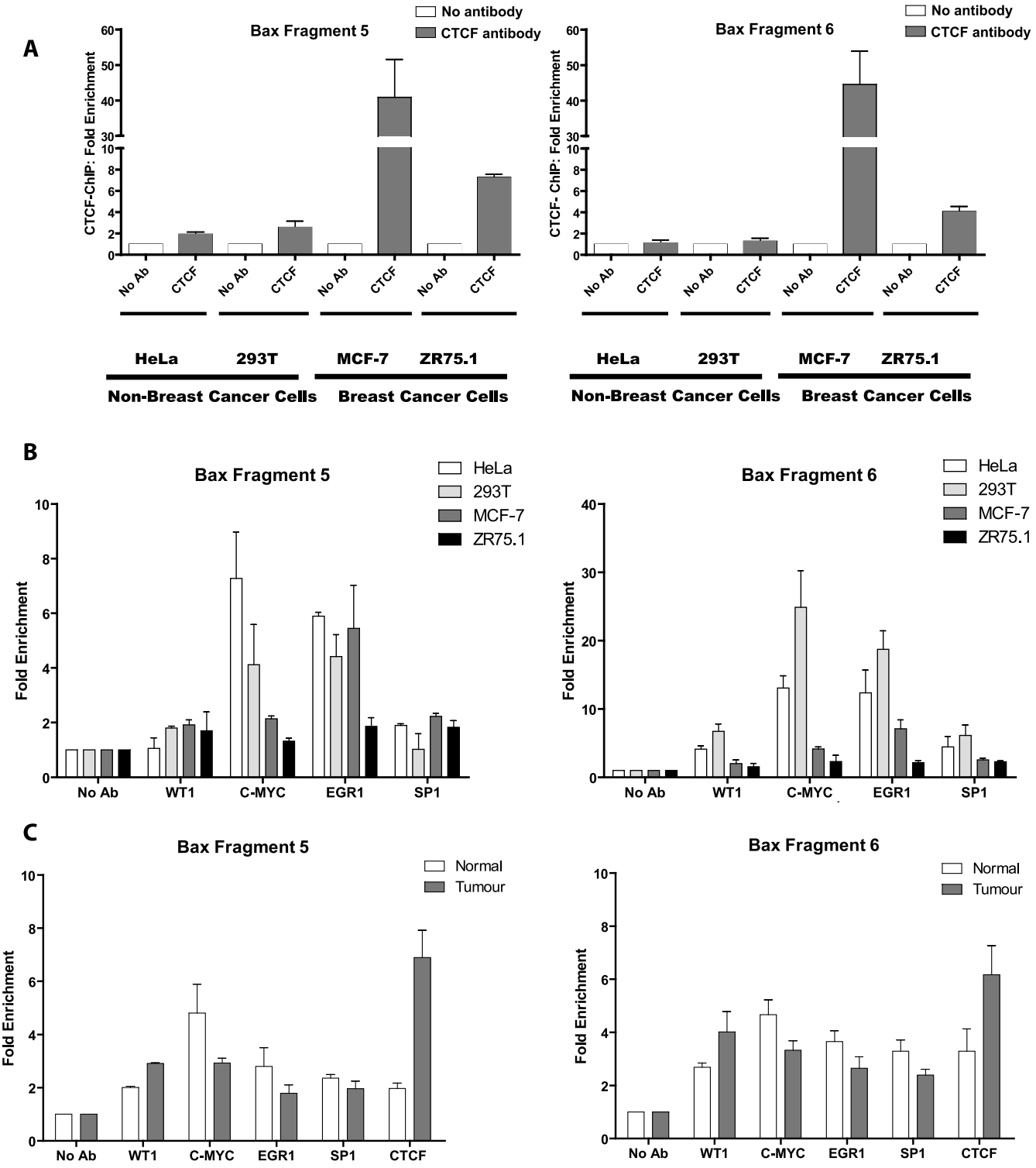

Figure 6. CTCF preferentially binds to the CTSs in the *Bax* promoter in breast cancer cells and tumors, whereas occupancy with other factors is enriched in non–breast cells and normal tissues. Cells or fresh tissues were prepared for ChIP and immunoprecipitated with the following antibodies: anti-CTCF, SP1, WT1, EGR1, and c-Myc [30]; DNA was extracted and qPCR was performed using primers specific to *Bax* fragment 5 or fragment 6 as described under Materials and Methods section. Results were calculated as the percentage of input chromatin precipitated at the region of interest and presented as fold change relative to the control ChIP experiment with no antibody (designated as 1.0). Experiments were performed in triplicate and the mean value is shown. Error bars indicate SDs. (A) Analysis of CTCF binding to the *Bax* promoter in breast and non–breast cell lines. (B) Analysis of CTCF, SP1, WT1, EGR1, and c-Myc binding to the *Bax* promoter in breast and non–breast cell lines. (C) Analysis of CTCF, SP1, WT1, EGR1, and c-Myc binding to the *Bax* promoter in normal and tumor breast tissues (specimen 1094). The rabbit polyclonal anti-CTCF antibody (Abcam) and Protein A-BioVyon gravity free flow columns (Porvair Technology) were used in these experiments [33].

is very difficult to ascertain which CTCF threshold levels would be necessary and sufficient to commit cells to apoptosis. Indeed, variations of CTCF levels were observed in apoptotic cells, which may be explained by different sensitivity of cells due to different physiological states (e.g., cell cycle). We also demonstrate that the previously described apoptotic events in breast cancer cells with reduced CTCF levels are mainly driven by overexpression of Bax. In these cells, simultaneously treated with CTCF siRNA and Bax siRNA, the levels of the cleaved PARP-1 fragment of 89 kDa are decreased and more viable cells are observed than in those transfected with the CTCF siRNA only. However, it should be noted that these Bax-independent pathways may also be involved, as the apoptotic events are not completely compensated by Bax knockdown (also see below).

The direct role of CTCF in the regulation of the *Bax* gene was supported by the identification of two CTSs within the *Bax* gene promoter ("CTS-1" in fragment 5 and "CTS-2" in fragment 6). While sequences within these fragments comply with the previously identified CTCF "consensus" motif [42], methylation interference assays in combination with mutational analysis will be necessary for precise identification of the contact nucleotides. This information will also be useful for accurate measurements of CTCF occupancy at each site by ChIP assays. Interestingly, both sites are located downstream of the transcription start site, which is characteristic for genes negatively regulated by CTCF [34,45]. The presence of negative CTCF-dependent elements within the *Bax* promoter was also confirmed in reporter assays: the reporter construct was repressed by the exogenously supplied CTCF in all the cell lines tested, breast and non-breast. The repressive function of CTCF in both cell types is not surprising as the transfected DNA lacks the appropriate chromatin environment, likely to be important for CTCF-specific function *in vivo* in a particular cell context.

We also found that the *Bax* gene was active in all cell lines and tissues tested. The DNA region containing the CTSs was also enriched with the marks characteristic for open chromatin and unmethylated in all specimens analyzed. Because only breast cancer cells were sensitive to CTCF depletion, we proposed a model of epigenetic regulation of *Bax* in different cell contexts, whereby different sets of transcription factors, activators and repressors, occupy the regulatory elements of the gene and control its function (Figure 8). We hypothesize that, in breast cancer cells, elevated levels of CTCF [11] favor preferential binding to the CTSs (Figure 8, *A* and *B*) by CTCF but not other transcription factors. Of note, in further support of the specific function of CTCF in breast cells is that overexpression of CTCF in non–breast cells does not lead to changes in Bax production or the increase of CTCF association with the CTSs. In non–breast cells and in normal breast tissues, less CTCF but more other factors bind to the *Bax* promoter. The composition and abundance of such factors may be different in these two contexts; this is indicated by differently positioned and sized circles (Figure 8, *C* and *D*). In contrast, in non–breast cells where removal of relatively small amounts of bound CTCF does not change the overall balance between negative and positive regulators, apoptosis does not occur (Figure 8*E*). In breast cancer cells, more CTCF is bound to *Bax*; following depletion, the negative influences of

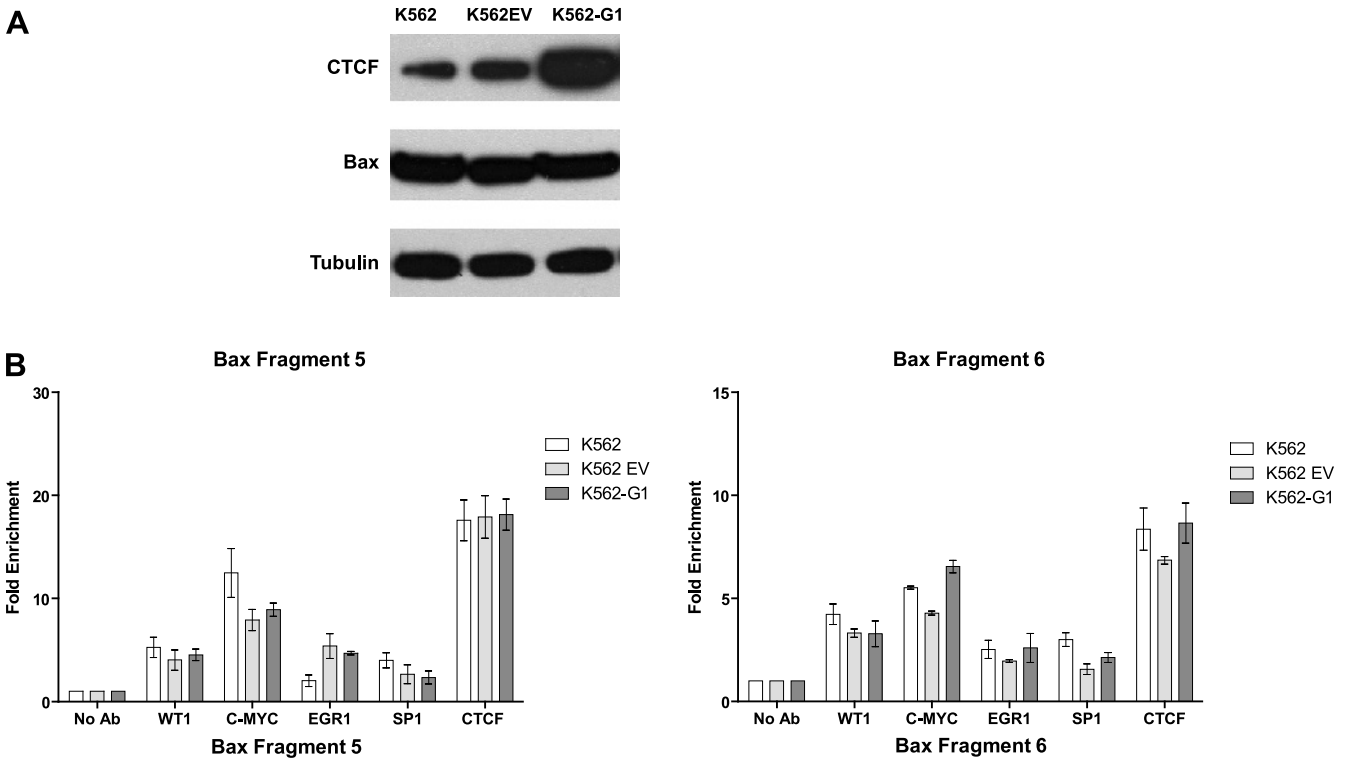

Figure 7. Binding of CTCF and other factors to the CTSs in the *Bax* promoter is similar in K562 cells ectopically overexpressing CTCF and in control K562 cells. (A) Western blot analysis of leukemia cells K562, K562EV, and K562-G1. Cellular extracts (20 μg of total protein) were loaded onto SDS-PAGE, separated, blotted, and probed with the anti-Bax antibody. The same membrane was stripped and reprobed subsequently with the anti-CTCF and α-tubulin antibodies (loading control). K562-G1 cells are cells overexpressing CTCF, K562 cells are original K562 unmodified cells, and K562EV cells are cells stably transfected with the backbone empty plasmid pcDNA3 [26]. (B) Analysis of CTCF, SP1, WT1, EGR1, and c-Myc binding to the *Bax* promoter in K562, K562EV, and K562-G1 cells.

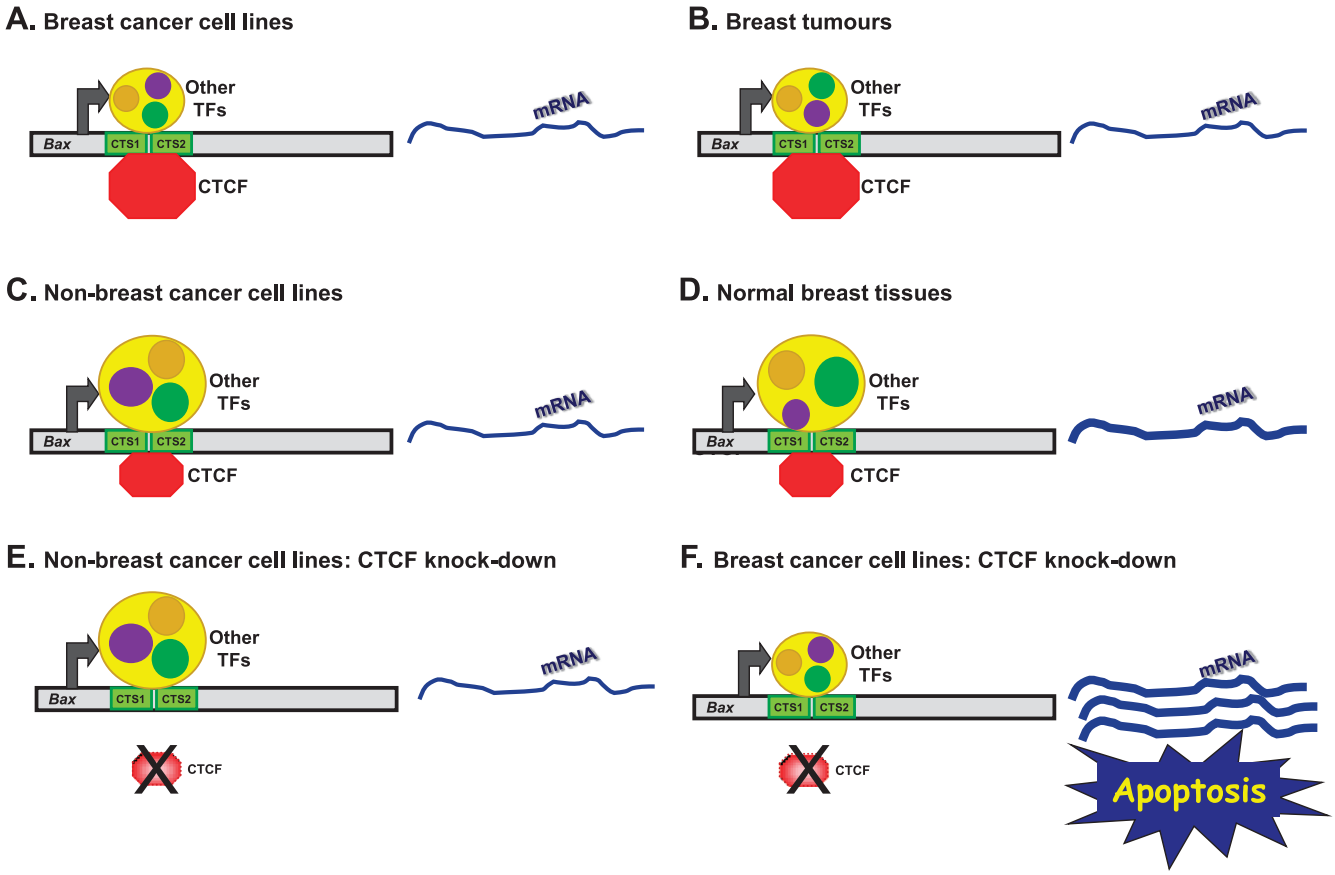

Figure 8. Model of the regulation of *Bax* gene by CTCF in different cell contexts. Horizontal gray bars depict the *Bax* gene promoter, two CTSs were represented by green boxes, and *Bax* mRNA is shown as a curved blue line; the thickness of the curves reflects mRNA levels. Octagons depict CTCF (red) and other transcription factors are shown inside the yellow circle. Different configurations of these factors in different cell contexts are indicated by repositioned circles. (A and B) Breast cancer cell lines and tissues, respectively: binding of CTCF is higher than other transcription factors. (C and D) Non–breast cancer cells and normal breast tissues, respectively: binding of other transcription factors is higher than CTCF. (E) Knockdown of CTCF in non–breast cell lines has no effect. (F) Knockdown of CTCF leads to activation of *Bax* and apoptosis in breast cancer cells. (For more detailed explanations, see main text.)

CTCF are counteracted leading to hyperactivation of *Bax* and apoptosis (Figure 8*F*). However, it must be acknowledged that transcriptional regulation of *Bax* may be more complex and involve other DNA elements and factors. Therefore, the proposed model should be further validated and refined, for example, by analyzing changes in other factors' binding following CTCF knockdown and using primary rather than established cell lines.

In this study, we provide evidence that the Bax-dependent pathways play a very important part in the regulation of *Bax* by CTCF in breast cancer cells and also the insight into the molecular mechanisms of this regulation. However, because of particular properties of CTCF (e.g., numerous binding sites and multiplicity of functions) [1–3], CTCF involvement in the regulation of apoptosis in breast cancer cells is likely to be more global and not limited to *Bax*. Indeed, this proposition was supported by the microarray and proteomics analyses that revealed differential expression of a number of apoptotic genes/proteins in breast cancer cells depleted for CTCF [48]. This project is the focus of our ongoing work, which will be described in a separate research article (C.F. Méndez-Catalá et al., manuscript in preparation).

Of note and in agreement with data elsewhere [46], the levels of *Bax* mRNA in normal breast tissues were significantly higher than in the corresponding tumors. In this study, this observation was confirmed for Bax protein. The presence of Bax at higher levels in normal tissues highlights the importance of active apoptotic processes for normal tissue functions. However, progressive loss of Bax and, as a consequence, apoptotic functions constitute the hallmarks of cancer in many tissues [49]. However, as illustrated by this investigation, the molecular mechanisms of *Bax* deregulation may vary in different tissues.

An interesting aspect of our previous [11] and current studies is that the regulatory effects of CTCF on *Bax* and possibly other apoptotic genes are likely to be p53 independent in breast cancer cell lines. Indeed, similar observations were made here using cell lines containing wild-type p53 (MCF-7) and mutant p53 (ZR75.1). This may be highly relevant to the observations that apoptosis can still occur through p53-independent apoptotic processes in human cancer cells that lack a functional p53 tumor suppressor protein [22]. The existence of such p53-independent apoptotic pathways opens up attractive perspectives for the development of anti–breast cancer therapies, independently of tumors' p53 status, which may be based on selective reduction of CTCF in breast cancer cells. Interestingly, our preliminary experiments demonstrate that the simultaneous treatment of breast cancer cells, in which CTCF is silenced, with chemotherapeutic agents of different classes, Taxol (antimicrotubule) and Mitoxantrone (DNA topoisomerase II inhibitor), increases the sensitivity of these cells to

the drugs, even at lower concentration of the drugs (Figure W10). This finding may be very useful in the design of new therapeutic strategies. Our current and future investigations aim to explore these avenues further.

Acknowledgments

We thank P. Flanagan for the *in vitro* translated DNA binding domain of CTCF and the full-length CTCF, D. Delgado for K562, K562EV, and K562-G1 cells, S. Brown and D. Cowieson from Porvair Filtration Group Ltd for the Protein A-BioVyon Gravity flow columns, I. Chernukhin for technical advice on ChIP and CTCF protein analyses, M. Docquier for technical advice on qPCR, and A. Angel for excellent technical assistance. We are also grateful to C. Chandrasekharan, K. Rooke, and K. Reeve for help with tissue collection and information and I. Seddon for specialist advice and expertise on breast tumor tissues.

References

[1] Ohlsson R, Lobanenkov V, and Klenova E (2010). Does CTCF mediate between nuclear organization and gene expression? *Bioessays* **32**, 37–50.

[2] Phillips JE and Corces VG (2009). CTCF: master weaver of the genome. *Cell* **137**, 1194–1211.

[3] Handoko L, Xu H, Li G, Ngan CY, Chew E, Schnapp M, Lee CW, Ye C, Ping JL, Mulawadi F, et al. (2011). CTCF-mediated functional chromatin interactome in pluripotent cells. *Nat Genet* **43**, 630–638.

[4] Fiorentino FP and Giordano A (2011). The tumor suppressor role of CTCF. *J Cell Physiol* **227**, 479–492.

[5] Recillas-Targa F, De La Rosa-Velazquez IA, Soto-Reyes E, and Benitez-Bribiesca L (2006). Epigenetic boundaries of tumour suppressor gene promoters: the CTCF connection and its role in carcinogenesis. *J Cell Mol Med* **10**, 554–568.

[6] Saldana-Meyer R and Recillas-Targa F (2011). Transcriptional and epigenetic regulation of the p53 tumor suppressor gene. *Epigenetics* **6**, 1068–1077.

[7] Rayess H, Wang MB, and Srivatsan ES (2011). Cellular senescence and tumor suppressor gene p16. *Int J Cancer* **130**, 1715–1725.

[8] Klenova EM, Morse HC III, Ohlsson R, and Lobanenkov VV (2002). The novel *BORIS+CTCF* gene family is uniquely involved in the epigenetics of normal biology and cancer. *Semin Cancer Biol* **12**, 399–414.

[9] Wallace JA and Felsenfeld G (2007). We gather together: insulators and genome organization. *Curr Opin Genet Dev* **17**, 400–407.

[10] Docquier F, Kita GX, Farrar D, Jat P, O'Hare M, Chernukhin I, Gretton S, Mandal A, Alldridge L, and Klenova E (2009). Decreased poly(ADP-ribosyl) ation of CTCF, a transcription factor, is associated with breast cancer phenotype and cell proliferation. *Clin Cancer Res* **15**, 5762–5771.

[11] Docquier F, Farrar D, D'Arcy V, Chernukhin I, Robinson AF, Loukinov D, Vatolin S, Pack S, Mackay A, Harris RA, et al. (2005). Heightened expression of CTCF in breast cancer cells is associated with resistance to apoptosis. *Cancer Res* **65**, 5112–5122.

[12] Cory S and Adams JM (2002). The Bcl2 family: regulators of the cellular life-or-death switch. *Nat Rev Cancer* **2**, 647–656.

[13] Garcia-Saez AJ (2012). The secrets of the Bcl-2 family. *Cell Death Differ* **19**, 1733–1740.

[14] van Delft MF and Huang DC (2006). How the Bcl-2 family of proteins interact to regulate apoptosis. *Cell Res* **16**, 203–213.

[15] Jurgensmeier JM, Xie Z, Deveraux Q, Ellerby L, Bredesen D, and Reed JC (1998). Bax directly induces release of cytochrome *c* from isolated mitochondria. *Proc Natl Acad Sci USA* **95**, 4997–5002.

[16] Loeb DM (2006). WT1 influences apoptosis through transcriptional regulation of Bcl-2 family members. *Cell Cycle* **5**, 1249–1253.

[17] Zagurovskaya M, Shareef MM, Das A, Reeves A, Gupta S, Sudol M, Bedford MT, Prichard J, Mohiuddin M, and Ahmed MM (2009). EGR-1 forms a complex with YAP-1 and upregulates Bax expression in irradiated prostate carcinoma cells. *Oncogene* **28**, 1121–1131.

[18] Mitchell KO, Ricci MS, Miyashita T, Dicker DT, Jin Z, Reed JC, and El-Deiry WS (2000). Bax is a transcriptional target and mediator of c-myc-induced apoptosis. *Cancer Res* **60**, 6318–6325.

[19] Miyashita T and Reed JC (1995). Tumor suppressor p53 is a direct transcriptional activator of the human *bax* gene. *Cell* **80**, 293–299.

[20] Cianfrocca R, Muscolini M, Marzano V, Annibaldi A, Marinari B, Levrero M, Costanzo A, and Tuosto L (2008). RelA/NF-κB recruitment on the *bax* gene promoter antagonizes p73-dependent apoptosis in costimulated T cells. *Cell Death Differ* **15**, 354–363.

[21] Pietsch EC, Sykes SM, McMahon SB, and Murphy ME (2008). The p53 family and programmed cell death. *Oncogene* **27**, 6507–6521.

[22] Peled A, Zipori D, and Rotter V (1996). Cooperation between p53-dependent and p53-independent apoptotic pathways in myeloid cells. *Cancer Res* **56**, 2148–2156.

[23] Zhivotovsky B and Orrenius S (2006). Carcinogenesis and apoptosis: paradigms and paradoxes. *Carcinogenesis* **27**, 1939–1945.

[24] Schelwies K, Sturm I, Grabowski P, Scherubl H, Schindler I, Hermann S, Stein H, Buhr HJ, Riecken EO, Zeitz M, et al. (2002). Analysis of p53/BAX in primary colorectal carcinoma: low BAX protein expression is a negative prognostic factor in UICC stage III tumors. *Int J Cancer* **99**, 589–596.

[25] Sturm I, Papadopoulos S, Hillebrand T, Benter T, Luck HJ, Wolff G, Dorken B, and Daniel PT (2000). Impaired BAX protein expression in breast cancer: mutational analysis of the BAX and the *p53* gene. *Int J Cancer* **87**, 517–521.

[26] Torrano V, Chernukhin I, Docquier F, D'Arcy V, Leon J, Klenova E, and Delgado MD (2005). CTCF regulates growth and erythroid differentiation of human myeloid leukemia cells. *J Biol Chem* **280**, 28152–28161.

[27] Flanagan L, Van Weelden K, Ammerman C, Ethier SP, and Welsh J (1999). SUM-159PT cells: a novel estrogen independent human breast cancer model system. *Breast Cancer Res Treat* **58**, 193–204.

[28] D'Arcy V, Pore N, Docquier F, Abdullaev ZK, Chernukhin I, Kita GX, Rai S, Smart M, Farrar D, Pack S, et al. (2008). BORIS, a paralogue of the transcription factor, CTCF, is aberrantly expressed in breast tumours. *Br J Cancer* **98**, 571–579.

[29] Farrar D, Rai S, Chernukhin I, Jagodic M, Ito Y, Yammine S, Ohlsson R, Murrell A, and Klenova E (2010). Mutational analysis of the poly(ADP-ribosyl)ation sites of the transcription factor CTCF provides an insight into the mechanism of its regulation by poly(ADP-ribosyl)ation. *Mol Cell Biol* **30**, 1199–1216.

[30] Pugacheva EM, Tiwari VK, Abdullaev Z, Vostrov AA, Flanagan PT, Quitschke WW, Loukinov DI, Ohlsson R, and Lobanenkov VV (2005). Familial cases of point mutations in the XIST promoter reveal a correlation between CTCF binding and pre-emptive choices of X chromosome inactivation. *Hum Mol Genet* **14**, 953–965.

[31] Abramoff MD, Magalhaes PJ, and Ram SJ (2004). Image processing with ImageJ. *Biophotonics Int* **11**, 36–42.

[32] Pfaffl MW (2001). A new mathematical model for relative quantification in real-time RT-PCR. *Nucleic Acids Res* **29**, e45.

[33] Chernukhin I, Kang SY, Brown S, Gretton S, Mendez-Catala CF, Cowieson D, and Klenova E (2011). BioVyon Protein A, an alternative solid-phase affinity matrix for chromatin immunoprecipitation. *Anal Biochem* **412**, 183–188.

[34] Filippova GN, Fagerlie S, Klenova EM, Myers C, Dehner Y, Goodwin G, Neiman PE, Collins SJ, and Lobanenkov VV (1996). An exceptionally conserved transcriptional repressor, CTCF, employs different combinations of zinc fingers to bind diverged promoter sequences of avian and mammalian c-myc oncogenes. *Mol Cell Biol* **16**, 2802–2813.

[35] van Meerloo J, Kaspers GJ, and Cloos J (2011). Cell sensitivity assays: the MTT assay. *Methods Mol Biol* **731**, 237–245.

[36] Nagata S (1997). Apoptosis by death factor. *Cell* **88**, 355–365.

[37] Chaitanya GV, Steven AJ, and Babu PP (2010). PARP-1 cleavage fragments: signatures of cell-death proteases in neurodegeneration. *Cell Commun Signal* **8**, 31.

[38] Lobanenkov VV, Nicolas RH, Adler VV, Paterson H, Klenova EM, Polotskaja AV, and Goodwin GH (1990). A novel sequence-specific DNA binding protein which interacts with three regularly spaced direct repeats of the CCCTC-motif in the 5′-flanking sequence of the chicken c-myc gene. *Oncogene* **5**, 1743–1753.

[39] Lobanenkov VV, Adler VV, Klenova EM, Nicolas RH, and Goodwin GH (1990). CCCTC-binding factor: a novel sequence specific protein which interacts with the 5′-flanking sequence of the chicken c-myc gene. In *Gene Regulation and AIDS: Transcriptional Activation, Retroviruses and Pathogenesis.* TS Papas (Ed). The Portfolio Publishing Co, London, United Kingdom. pp. 45–66.

[40] Ohlsson R, Renkawitz R, and Lobanenkov V (2001). CTCF is a uniquely versatile transcription regulator linked to epigenetics and disease. *Trends Genet* **17**, 520–527.

[41] Barski A, Cuddapah S, Cui K, Roh TY, Schones DE, Wang Z, Wei G, Chepelev I, and Zhao K (2007). High-resolution profiling of histone methylations in the human genome. *Cell* **129**, 823–837.

[42] Kim TH, Abdullaev ZK, Smith AD, Ching KA, Loukinov DI, Green RD, Zhang MQ, Lobanenkov VV, and Ren B (2007). Analysis of the vertebrate insulator protein CTCF-binding sites in the human genome. *Cell* **128**, 1231–1245.

[43] Cuddapah S, Jothi R, Schones DE, Roh TY, Cui K, and Zhao K (2009). Global analysis of the insulator binding protein CTCF in chromatin barrier regions reveals demarcation of active and repressive domains. *Genome Res* **19**, 24–32.

[44] Chen X, Xu H, Yuan P, Fang F, Huss M, Vega VB, Wong E, Orlov YL, Zhang W, Jiang J, et al. (2008). Integration of external signaling pathways with the core transcriptional network in embryonic stem cells. *Cell* **133**, 1106–1117.

[45] Renaud S, Loukinov D, Bosman FT, Lobanenkov V, and Benhattar J (2005). CTCF binds the proximal exonic region of hTERT and inhibits its transcription. *Nucleic Acids Res* **33**, 6850–6860.

[46] Bargou RC, Wagener C, Bommert K, Mapara MY, Daniel PT, Arnold W, Dietel M, Guski H, Feller A, Royer HD, et al. (1996). Overexpression of the death-promoting gene bax-alpha which is downregulated in breast cancer restores sensitivity to different apoptotic stimuli and reduces tumor growth in SCID mice. *J Clin Invest* **97**, 2651–2659.

[47] Sacha T, Zawada M, Hartwich J, Lach Z, Polus A, Szostek M, Zdzi Owska E, Libura M, Bodzioch M, Dembinska-Kiec A, et al. (2005). The effect of β-carotene and its derivatives on cytotoxicity, differentiation, proliferative potential and apoptosis on the three human acute leukemia cell lines: U-937, HL-60 and TF-1. *Biochim Biophys Acta* **1740**, 206–214.

[48] Méndez-Catalá CF (2011). *Investigation into the molecular mechanisms of the anti-apoptotic function of CTCF in breast cancer cells*. PhD thesis. University of Essex, United Kingdom.

[49] Burns TF and El-Deiry WS (2003). Cell death signaling in malignancy. *Cancer Treat Res* **115**, 319–343.

Supplemental Materials and Methods

Real-time RT-PCR: Conditions and Primers

Sequences of the primers used were as follows: *TBP* (TATA Binding Protein), (For) 5′-gcccgaaacgccgaatata-3′ and (Rev) 5′-cgtggctcttcttatcctcatga-3′; *glyceraldehyde-3-phosphate dehydrogenase* (*GAPDH*), (For) 5′-accacagtccatgccatcac-3′ and (Rev) 5′-tccaccaccctgttgctgta-3′; *CTCF*, (For) 5′-agatcatgatttccagccca-3′ and (Rev) 5′-tgtgacagttcatgtgcaaga-3′ [1] and *Bax*, (For) 5′-ctggacagtaacatggagctg-3′ and (Rev) 5′-cactcggaaaaagacctctcg-3′ [2]; *cyclophilin B*, (For) 5′-tggcacaggaggaaagagcatc-3′ and (Rev) 5′-aaagggcttctccacctcgatc-3′ [3]. Each PCR generated only the expected specific amplicon, as shown by the melting temperature profiles of final products (data not shown). The comparative C_t method was used to assess relative changes in *mRNA* levels [4]. Thermal cycling conditions were given as follows: 95°C for 10 minutes, followed by 40 cycles of amplification, consisting of 94°C for 10 seconds, 60°C for 20 seconds, and 72°C for 20 seconds followed by data acquisition. For *cyclophilin B*, the PCR conditions were given as follows: initial denaturation for 10 minutes at 95°C; cycle (×40): 95°C for 15 seconds, 60°C for 30 seconds, 72°C for 20 seconds, final elongation at 72°C for 5 seconds, followed by data acquisition.

ChIP: Conditions and Primers for Real-Time PCR

Thermal cycling conditions were given as follows: 95°C for 10 minutes followed by 35 or 40 cycles of amplification (95°C for 15 seconds and 60°C for 20 seconds). Primers used for ChIP were given as follows: *Bax* fragment 5, (For) 5′-ggcattagagctgcgattgg-3′ and (Rev) 5′-cgtgacgggaccaaacctccc-3′; *Bax* fragment 6, (For) 5′-gggagcgaggcaggtgcggt-3′ and (Rev) 5′-cacgtgacccgggcgcgct-3′; TATA box of *Bax* gene, (For) 5′-ttgctagatccaggtctctgca-3′ and (Rev) 5′-agcgcagaaggaattagcaagt-3′.

DNase I Footprinting: Primers and Conditions

The DNase I footprinting analysis was performed according to a previously described protocol [5] with the *in vitro* translated, full-length CTCF and two CTCF binding fragments 5 and 6 that were amplified by PCR. The following primers were used for PCR amplification: forward 5′-acttgctaattccttctgcgg 3′ and reverse 5′-cgtgaccgcacctgcctcgct primers from the plasmid pBax5-pDrive (PCR fragment 5 cloned into pDrive vector; Qiagen) and forward 5′-ggacagtcacgtgacgggacc 3′ and reverse 5′-gccgcctctcgccgggtccgcg 3′ primers from the plasmid pBax6-pDrive (PCR fragment 6 cloned into pDrive vector). The amplification protocol was given as follows: denaturation at 95°C for 5 minutes, followed by 35 cycles at 95°C for 30 seconds, 64°C for 30 seconds, 72°C for 1 minute, and final extension at 72°C for 10 minutes. The fragments were labeled at their 5′ ends on either the top or the bottom strand. Following gel purification, the fragments were incubated with CTCF and then partially digested with DNase I.

Bisulfite Conversion of DNA

Genomic DNA (500 ng) was treated using the EZ DNA Methylation-Gold Kit (Zymo Research, Irvine, CA) as recommended by the manufacturer. The primers used for amplification of *Bax* promoter from the treated DNA were as follows: (Forward) 5′-ggtgtttggataaatgaaggtat-3′ and (Reverse) 5′-aaaatttctacccctcaatactta-3′. PCR fragments were ligated into the TOPO TA cloning vector (Invitrogen, Carlsbad, CA). Following transformation, plasmids from individual colonies were isolated and the *Bax* promoter was sequenced (GeneService, Cambridge, United Kingdom). Single clone sequences were analyzed with the BiQ Analyzer software (Max-Planck-Institut für Informatik, Saarbrücken, Germany) [6].

Drug Treatments

Taxol (paclitaxel) and Mitoxantrone (both obtained from Sigma-Aldrich) were diluted in DMSO (Taxol) or water (Mitoxantrone) and stored according to the manufacturer's instructions. MCF-7 and ZR75.1 breast cancer cells were transfected with 50 pM CTCF siRNA, 50 pM non-target siRNA, or transfection reagent only ("Mock"). Twenty-four hours post-transfection, cells were treated with trypsin, counted, replated onto 96-well plates (5×10^4 per well), and incubated overnight. After a total of 48 hours post-transfection, the medium was changed to the phenol-free RPMI containing Taxol at different concentrations (indicated in the figure) and left for further 24 hours. Triplicate wells were used for each concentration. Cell survival was measured using MTT assay (Sigma-Aldrich) as described in the manufacturer's manual. Briefly, 20 μl of 5 mg/ml MTT was added to the wells and cells were incubated at 37°C for 3.5 hours. The medium was then removed, and 150 μl of the MTT solution was added to the cells for further incubation for 15 minutes at room temperature with shaking. The OD_{590} and OD_{620} were read using Versamax plate reader. Control cells were treated with DMSO (0.1%) or water alone. Cell survival was calculated as a percent of control (DMSO-treated in experiments with Taxol or water-treated in experiments with Mitoxantrone) cells as described previously [7].

Supplemental References

[1] Roberts J, Scott AC, Howard MR, Breen G, Bubb VJ, Klenova E, and Quinn JP (2007). Differential regulation of the serotonin transporter gene by lithium is mediated by transcription factors, CCCTC binding protein and Y-box binding protein 1, through the polymorphic intron 2 variable number tandem repeat. *J Neurosci* **27**, 2793–2801.

[2] Wang X and Seed B (2003). A PCR primer bank for quantitative gene expression analysis. *Nucleic Acids Res* **31**, e154.

[3] Koh SW, Guo Y, Bernstein SL, Waschek JA, Liu X, and Symes AJ (2007). Vasoactive intestinal peptide induction by ciliary neurotrophic factor in donor human corneal endothelium *in situ*. *Neurosci Lett* **423**, 89–94.

[4] Pfaffl MW (2001). A new mathematical model for relative quantification in real-time RT-PCR. *Nucleic Acids Res* **29**, e45.

[5] Pugacheva EM, Tiwari VK, Abdullaev Z, Vostrov AA, Flanagan PT, Quitschke WW, Loukinov DI, Ohlsson R, and Lobanenkov VV (2005). Familial cases of point mutations in the XIST promoter reveal a correlation between CTCF binding and pre-emptive choices of X chromosome inactivation. *Hum Mol Genet* **14**, 953–965.

[6] Bock C, Reither S, Mikeska T, Paulsen M, Walter J, and Lengauer T (2005). BiQ Analyzer: visualization and quality control for DNA methylation data from bisulfite sequencing. *Bioinformatics* **21**, 4067–4068.

[7] van Meerloo J, Kaspers GJ, and Cloos J (2011). Cell sensitivity assays: the MTT assay. *Methods Mol Biol* **731**, 237–245.

[8] Abramoff MD, Magalhaes PJ, and Ram SJ (2004). Image processing with ImageJ. *Biophotonics Int* **11**, 36–42.

[9] Docquier F, Kita GX, Farrar D, Jat P, O'Hare M, Chernukhin I, Gretton S, Mandal A, Alldridge L, and Klenova E (2009). Decreased poly(ADP-ribosyl)ation of CTCF, a transcription factor, is associated with breast cancer phenotype and cell proliferation. *Clin Cancer Res* **15**, 5762–5771.

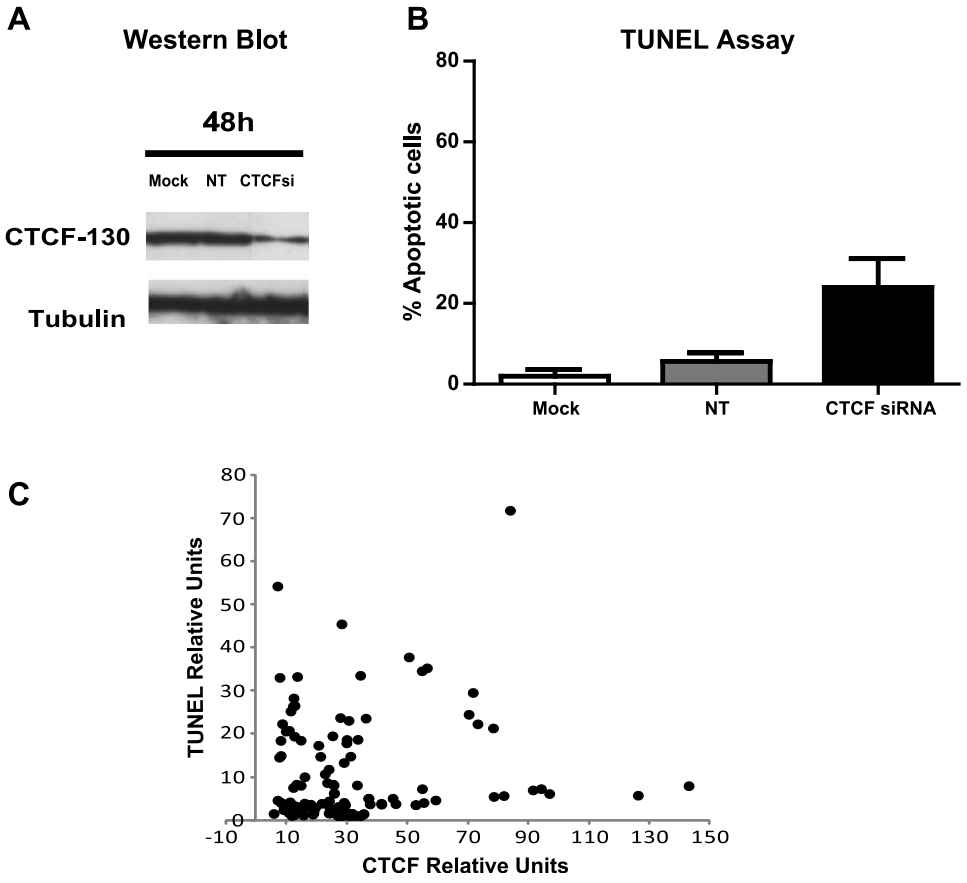

Figure W1. Transient knockdown of CTCF by CTCF siRNA induces apoptotic cell death in breast cancer cells, MCF-7. (A) Levels of CTCF are reduced in breast cancer cells, MCF-7, treated with the Hs_CTCF_4 siRNA as shown by Western blot analysis. Cells (2.5×10^5) were transfected with 50 pM target Hs_CTCF_4 siRNA (CTCF siRNA, "CTCF"), non-target siRNA ("NT"), or transfection reagent only ("Mock"). Forty-eight hours post-transfection, cells were collected, cellular extracts were prepared, and equal amounts (40 μg) of total protein were loaded onto SDS-PAGE. Samples were electrophoretically separated, blotted, and probed with the mouse monoclonal anti-CTCF antibody (BD Biosciences). The membrane was reprobed with the anti–α-tubulin antibody, which served as an internal control for protein loading. (B) Apoptotic cell death is induced by CTCF knockdown with the CTCF siRNA in breast cancer cells, MCF-7. Cells (2.5×10^5) were transiently transfected with 50 pM CTCF siRNA, non-target siRNA ("NT"), or transfection reagent only ("Mock"), and apoptotic cell death was assessed by TUNEL assay. The percentage of TUNEL-positive cells was calculated 48 hours after transfection. The results represent the mean values with the SDs (error bars) of three independent experiments. (C) Images were additionally analyzed using the ImageJ software [8]. The values were measured for CTCF and TUNEL staining in 100 cells; and the mean values for fluorescence were normalized by subtracting the background values. The results are presented as a scatter plot.

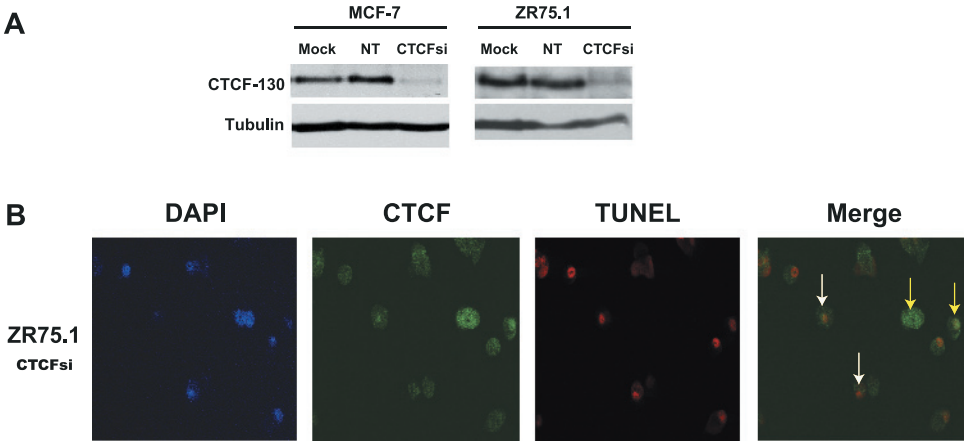

Figure W2. Transient knockdown of CTCF by SMARTpool CTCF siRNA induces apoptotic cell death in breast cancer cells. (A) Levels of CTCF are reduced in the breast cancer cells following CTCF knockdown, as shown by Western blot analysis. Breast cancer MCF-7 (2.5×10^5) and ZR75.1 (2.5×10^5) cells were transfected with 50 pM SMARTpool siRNA (CTCF siRNA, "CTCF"), 50 pM non-target siRNA ("NT"), or transfection reagent only ("Mock"). Forty-eight hours post-transfection, cells were collected, cellular extracts were prepared, and equal amounts (40 μg) of total protein were loaded onto SDS-PAGE. Samples were electrophoretically separated, blotted, and probed with the mouse monoclonal anti-CTCF antibody (BD Biosciences). The membrane was reprobed with the anti–α-tubulin antibody, which served as an internal control for protein loading. (B) Lower CTCF levels are associated with apoptotic death in breast cancer cells, ZR75.1. Cells (2.5×10^5) were transfected with 50 pM SMARTpool CTCF siRNA and analyzed by immunofluorescence staining with the anti-CTCF antibody (FITC, green fluorescence). Apoptotic cell death was assessed by TUNEL staining (TMR, red fluorescence). Nuclei were visualized by DAPI. Merge, overlay of the CTCF and TUNEL staining. TUNEL-positive (apoptotic) cells with low CTCF levels are indicated by white arrows. The TUNEL-negative cells with high levels of CTCF are indicated by yellow arrows.

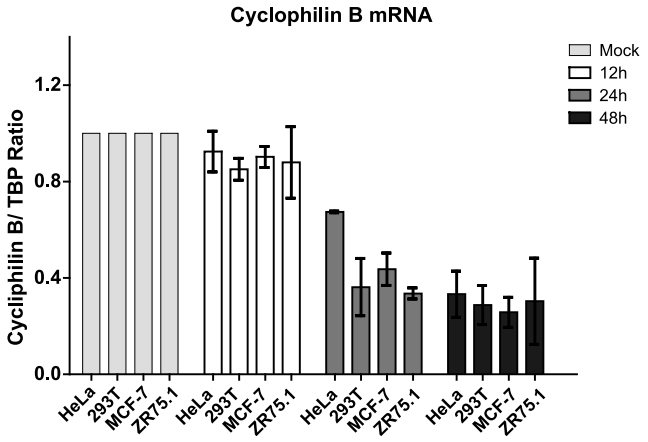

Figure W3. Transfection with the *cyclophilin B* siRNA leads to the reduction of the *cyclophilin B* mRNA levels in non–breast (HeLa and 293T) and breast cancer (MCF-7 and ZR75.1) cell lines. Cells were transfected with 50 pM *cyclophilin B* siRNA and collected 12, 24, and 48 hours post-transfection. The reagent-only ("Mock") reaction was used as control. The total RNA was extracted and analyzed by RT-qPCR. The expression of *cyclophilin B* was normalized to *TBP* mRNA expression, and the comparative C_t method ($\Delta\Delta C_t$) was used to calculate relative *cyclophilin B* mRNA levels. Columns represent fold change of *cyclophilin B*/*TBP* relative to mock-transfected cells (designated as 1.0). For each sample, measurements were performed at least in triplicates; error bars represent SDs.

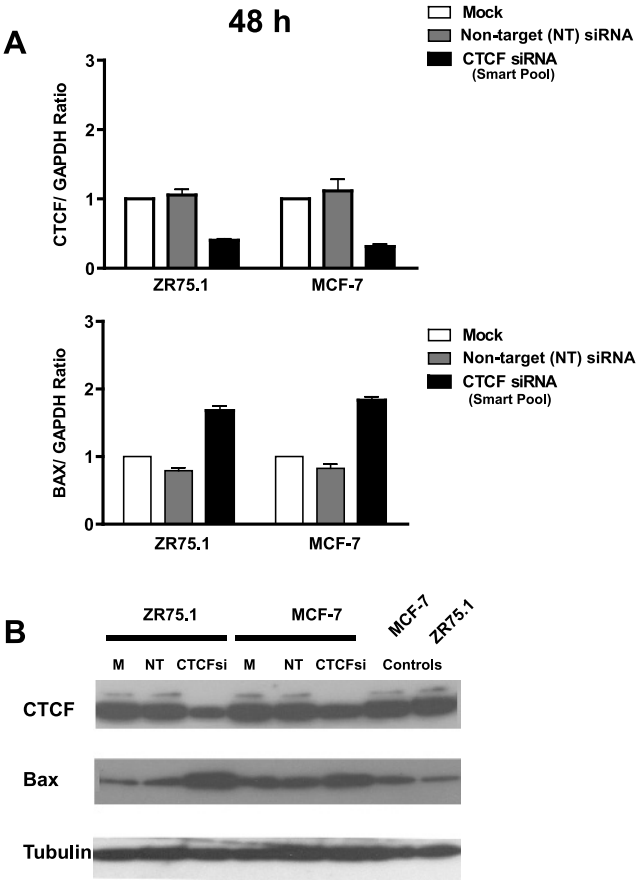

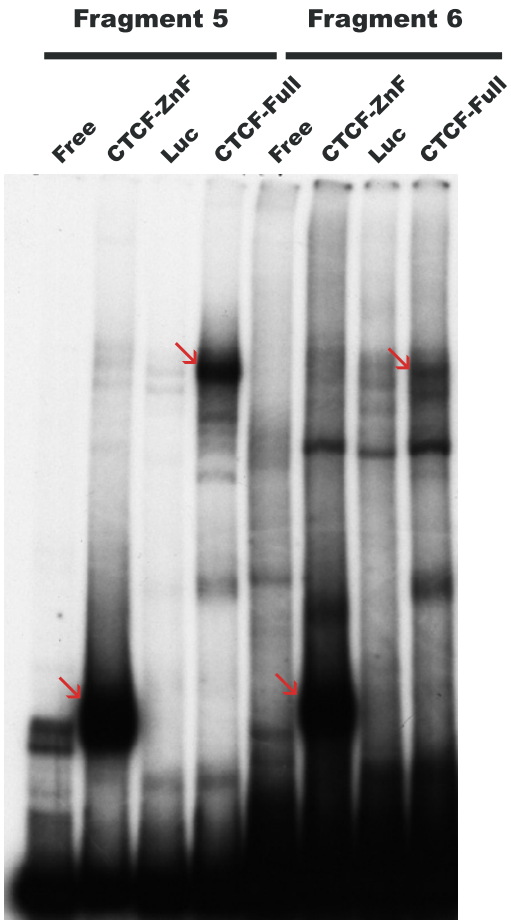

Figure W4. Levels of *Bax* mRNA and Bax protein increase in breast cancer cells following CTCF knockdown by the CTCF–SMARTpool siRNA. (A) Analysis of *Bax* mRNA. Breast cancer ZR75.1 (2.5×10^5) and MCF-7 (2.5×10^5) cells were transfected with 50 pM CTCF–SMARTpool siRNA, non-target siRNA (control), or transfection reagent only ("Mock") and harvested 48 hours post-transfection. Total RNA was prepared and analyzed by RT-qPCR. The expression levels of *CTCF* (upper panel) and *Bax* mRNA (lower panel) were calculated using the comparative C_t method ($\Delta\Delta C_t$) and normalized to *GAPDH* mRNA expression, representing fold change of *CTCF*/*GAPDH* mRNA or *Bax*/*GAPDH* levels relative to mock-transfected cells (designated as 1.0). For each sample, measurements were done at least in triplicates. Columns, mean mRNA/*GAPDH* relative level values. Bars, SDs. The difference in *CTCF* mRNA and *Bax* mRNA levels between cells treated with CTCF siRNA and control (non-target, NT) siRNA was statistically significant ($P \leq 0.01$). (B) Analysis of Bax protein levels. Following transfection as described above, cells were lysed, proteins separated by SDS-PAGE, blotted, and analyzed by Western blot analysis using CTCF, Bax, and α-tubulin (loading control) antibodies. Abbreviations: CTCFsi, CTCF siRNA; NT, non-target siRNA; M, transfection reagent only ("Mock"); two controls in the right lanes are extracts from untreated cells.

Figure W5. The full-length CTCF binds to fragments 5 and 6 within the promoter-proximal region of human *Bax* gene in the EMSA. EMSA analysis of CTCF binding to two overlapping fragments, 5 and 6, of the human *Bax* promoter. The DNA fragments were end-labeled with ^{32}P, and EMSA analyses were performed as described under Materials and Methods section. The *in vitro* translated 11-Zn-finger domain of CTCF (CTCF-ZnF), full-length CTCF (CTCF-Full), and luciferase (control, Luc) were used to assess specific and non-specific binding to the DNA. Free, free probe. Specific ZF-CTCF-DNA and CTCF-DNA complexes are indicated by red arrows.

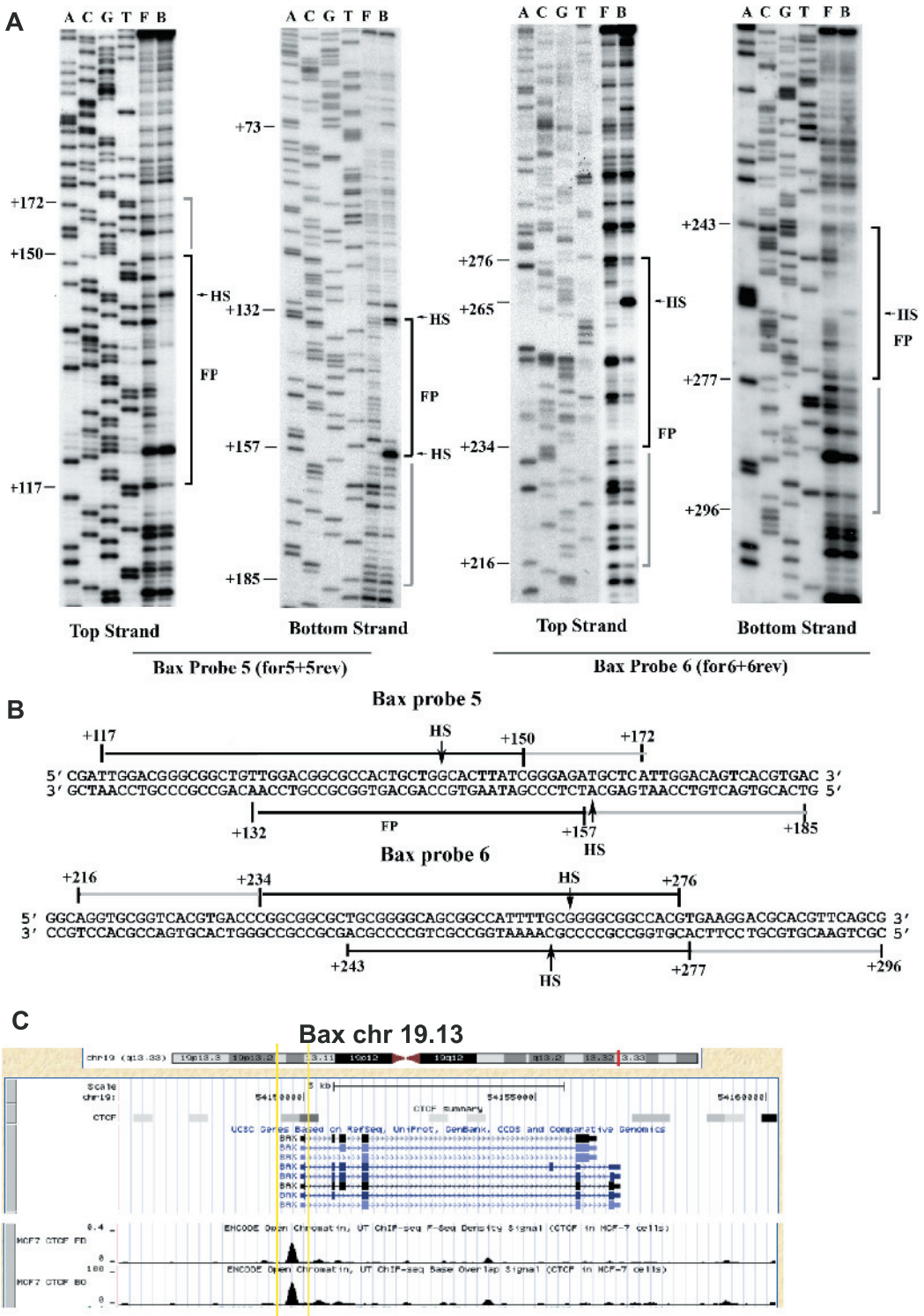

Figure W6. Footprinting analysis of CTCF binding to fragments 5 and 6 of the *Bax* gene promoter. (A) The 5′-^{32}P end-labeled fragments containing promoter regions between +24 and +226 (fragment 5) and +174 and +358 (fragment 6) downstream of the transcription start site were used as probes in the binding reaction with *in vitro* translated full-length CTCF. ACGT, the Maxam-Gilbert sequencing reactions; F, free probe; B, bound probe (reaction with CTCF). The strongly and weakly protected regions are indicated by black and gray lines, respectively. HS, hypersensitive sites; FP, footprint. Coordinates of the binding sites: chr19: 54,149,742 to 54,149,922. Coordinates are from the UCSC genome browser. (B) The sequences of the two CTCF bound fragments 5 and 6 within *Bax* promoter region. The lines on the top and bottom of double-stranded DNA sequences summarize the CTCF footprint on the top and bottom strands, respectively. (C) Analysis of the ChIP-seq data for CTCF binding in MCF-7 cells in the UCSC genome browser [http://genome.ucsc.edu/ (NCBI36/ hg18)]. Enrichment in CTCF is detected in the regions where CTSs in the *Bax* promoter were mapped (boxed in yellow). Coordinates mapped by ChIP-Seq: chr19: 54,149,575 to 54,149,958. (D) The maps depicted in C are shown at higher resolution. The positions of the transcription start site and translation start are indicated by the green and red arrows, respectively; the positions of the sites are given in brackets. Locations of fragments 5 and 6 are shown on the expanded maps below.

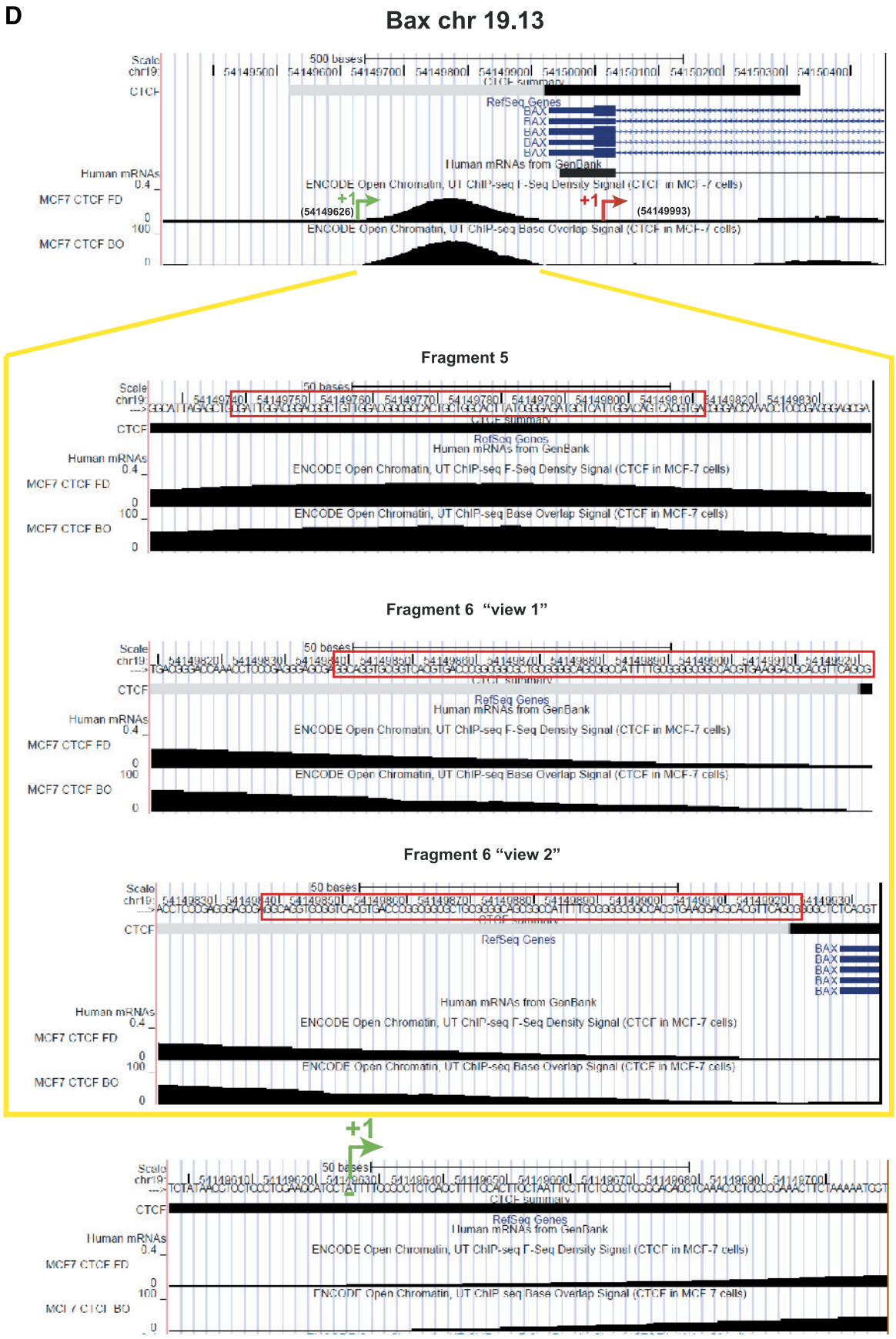

Figure W6. (*continued*).

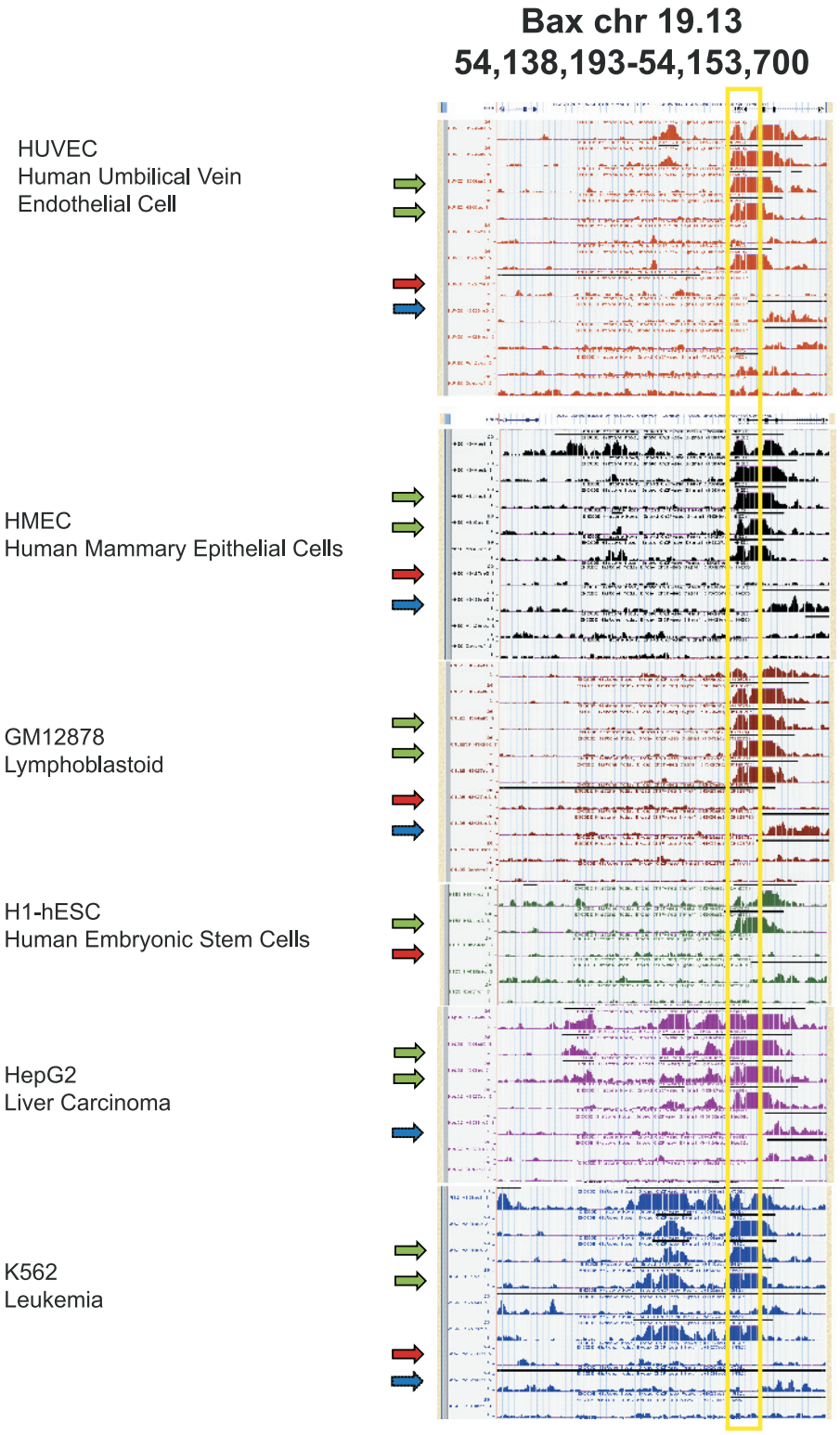

Figure W7. Open chromatin configuration is detected in the regions containing CTSs in the *Bax* promoter (boxed in yellow, coordinates are shown on top of the diagram) in a variety of breast and non–breast cells: analysis of the ChIP-seq data in the UCSC genome browser [http://genome.ucsc.edu/ (NCBI36/hg18)]. Typical examples are shown; they include HUVEC (human umbilical vein endothelial cell), HMEC (human mammary epithelial cells), GM12878 (lymphoblastoid), H1-hESC (human embryonic stem cells), HepG2 (liver carcinoma), and K562 (leukemia). Green arrows, histone marks associated with open chromatin; red arrows, histone marks associated with closed chromatin; blue arrows, dual histone marks (open and close chromatin).

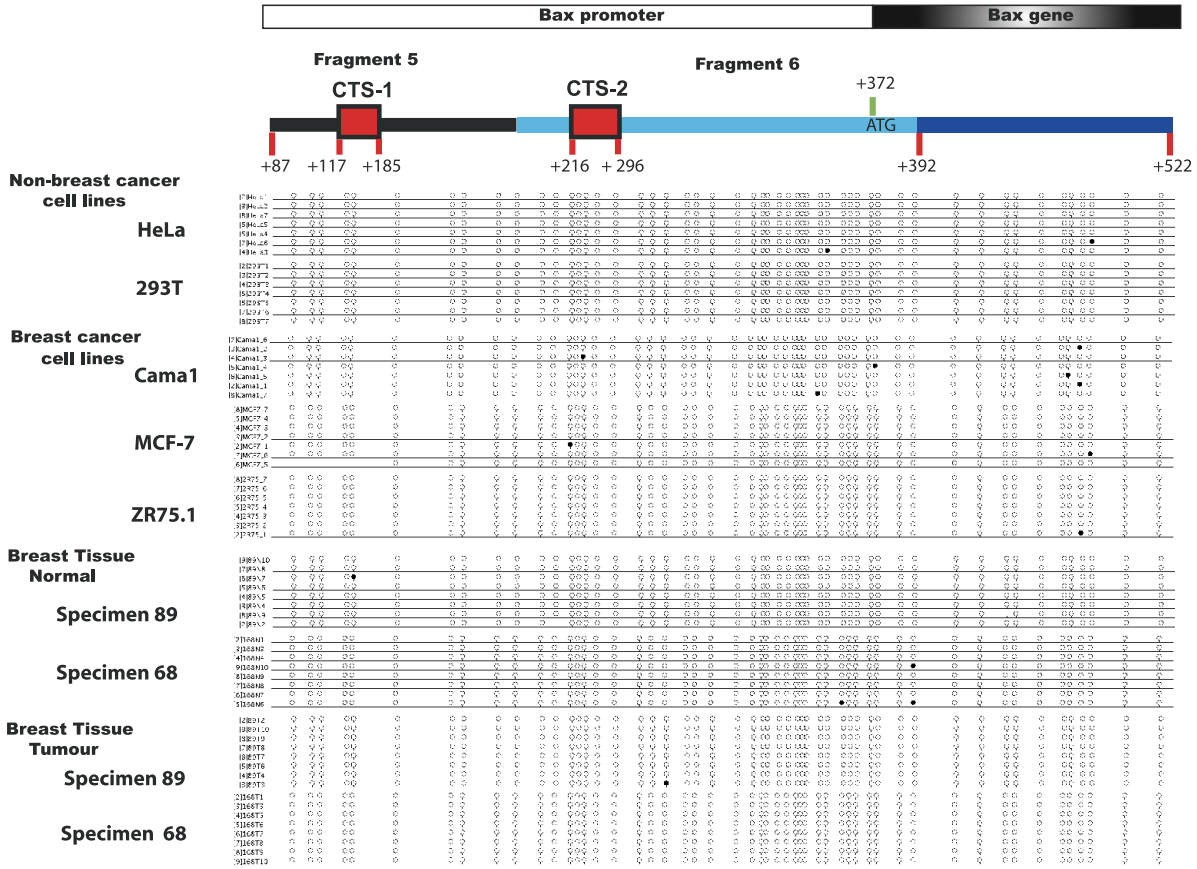

Figure W8. The *Bax* promoter is unmethylated in breast and non–breast cells and in normal and tumor breast tissues. As described under the Supplemental Materials and Methods section, genomic DNA (500 ng) from non–breast (HeLa and 293T) and breast (Cama1, MCF-7, and ZR.75.1) cell lines, two tumors (89T and 68T), and paired peripheral to tumors (89N and 68N) was purified, treated with bisulfate, amplified by PCR, and cloned. The plasmids from individual colonies were isolated and the *Bax* promoter was sequenced. DNA methylation status of CpG islands within fragments 5 and 6 is indicated as lollipop figures. Filled lollipops refer to methylated sites; open lollipops refer to unmethylated sites.

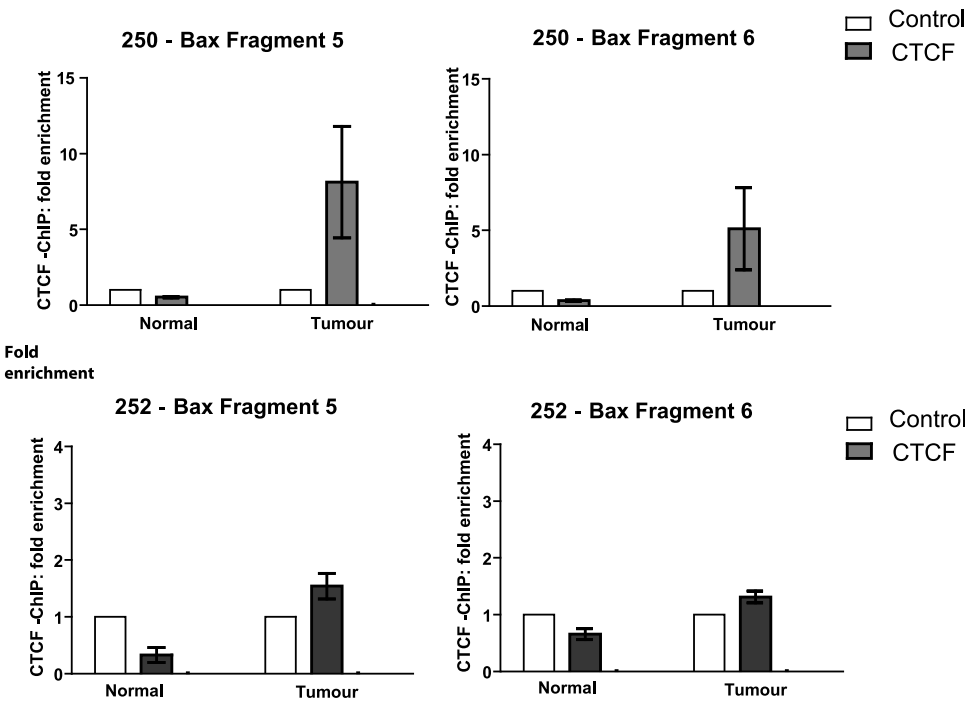

Figure W9. The CTSs are enriched with CTCF in breast cancer cells compared with normal breast and non–breast cancer cells. Analysis of CTCF binding to the *Bax* promoter in normal and tumor breast tissues (specimens 250 and 252, upper and lower panels, respectively) using ChIP assays. Cells were fixed with 1% formaldehyde to cross-link protein-DNA interactions and sonicated, and DNA-protein complexes were immunoprecipitated with the rabbit polyclonal anti-CTCF antibody (Abcam) [9]. The DNA was extracted and real-time PCR was performed using primers specific to *Bax* fragment 5 or fragment 6 as described under Materials and Methods section. Results were calculated as the percentage of input chromatin precipitated at the region of interest and presented as fold change relative to the control ChIP experiment with no antibody (designated as 1.0). Experiments were performed in triplicate, and the mean value is shown. Error bars indicate SDs.

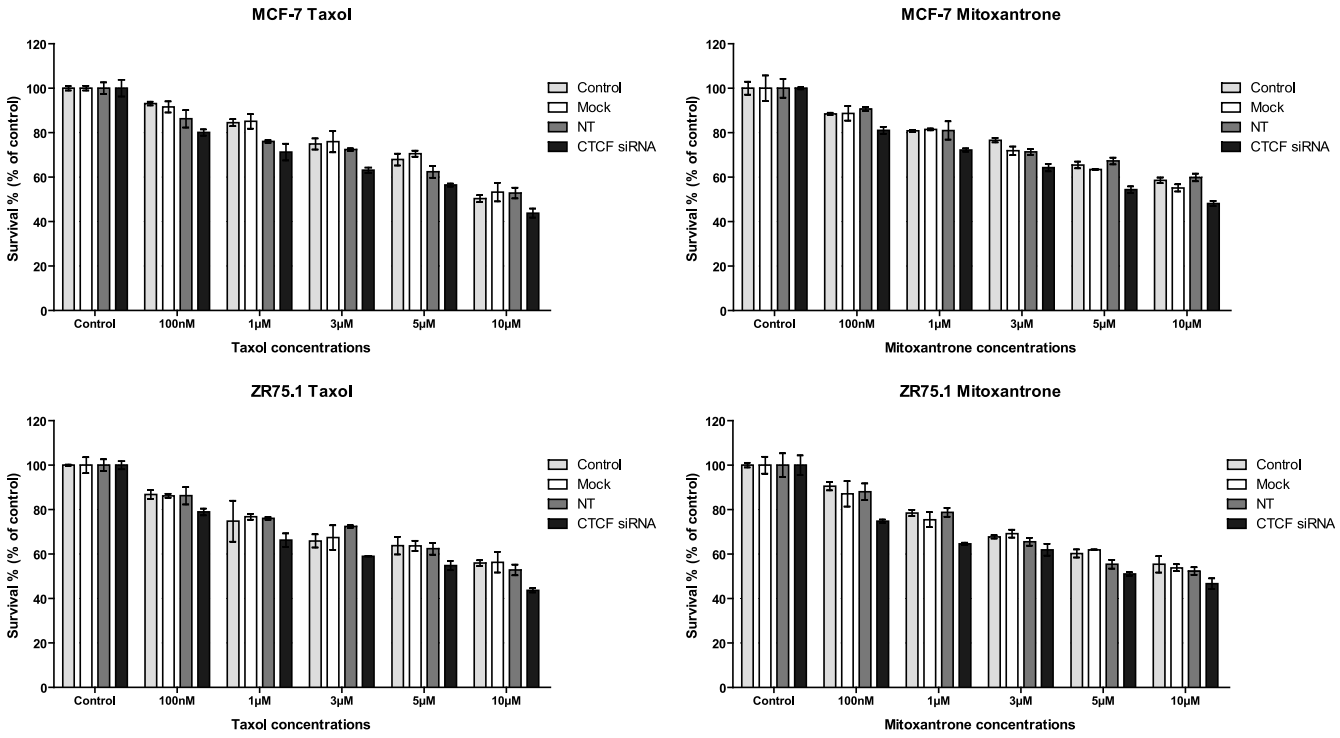

Figure W10. Cytotoxic effect of Taxol (paclitaxel) and Mitoxantrone in MCF-7 and ZR75.1 breast cancer cells. MCF-7 and ZR75.1 cells were transfected with 50 pM CTCF siRNA, 50 pM non-target siRNA, or transfection reagent only ("Mock"). Cells were treated with trypsin (24 hours post-transfection), counted, replated onto 96-well plates (5×10^4 per well), and incubated overnight. After a total of 48 hours post-transfection, the medium was changed to the phenol-free RPMI containing the drugs at the indicated concentrations and left for further 24 hours. Cell survival was measured using MTT assay (see Supplemental Materials and Methods section for details). Control cells were treated with DMSO (0.1%) or water alone. Cell survival was calculated as a percent of control (DMSO-treated in experiments with Taxol or water-treated in experiments with Mitoxantrone) cells as described previously [7]. The results represent the mean values with the SDs (error bars) of three independent experiments. The difference in the survival of cells treated with Taxol or Mitoxantrone at all concentrations was significantly less for cells transfected with the CTCF siRNA compared with other conditions ($P \leq 0.01$). Abbreviations: CTCFsi, CTCF siRNA; NT, non-target-siRNA; Mock, transfection reagent only; C, control (cells only).